

Article

## Exploiting the 4-Phenylquinazoline Scaffold for the Development of High Affinity Fluorescent Probes for the Translocator Protein (TSPO)

Ciro Milite, Elisabetta Barresi, Eleonora Da Pozzo, Barbara Costa, Monica Viviano, Amalia Porta, Anna Messere, Gianluca Sbardella, Federico Da Settimo, Ettore Novellino, Sandro Cosconati, Sabrina Castellano, Sabrina Taliani, and Claudia Martini

*J. Med. Chem.*, **Just Accepted Manuscript** • DOI: 10.1021/acs.jmedchem.7b01031 • Publication Date (Web): 31 Aug 2017

Downloaded from <http://pubs.acs.org> on September 4, 2017

### Just Accepted

“Just Accepted” manuscripts have been peer-reviewed and accepted for publication. They are posted online prior to technical editing, formatting for publication and author proofing. The American Chemical Society provides “Just Accepted” as a free service to the research community to expedite the dissemination of scientific material as soon as possible after acceptance. “Just Accepted” manuscripts appear in full in PDF format accompanied by an HTML abstract. “Just Accepted” manuscripts have been fully peer reviewed, but should not be considered the official version of record. They are accessible to all readers and citable by the Digital Object Identifier (DOI®). “Just Accepted” is an optional service offered to authors. Therefore, the “Just Accepted” Web site may not include all articles that will be published in the journal. After a manuscript is technically edited and formatted, it will be removed from the “Just Accepted” Web site and published as an ASAP article. Note that technical editing may introduce minor changes to the manuscript text and/or graphics which could affect content, and all legal disclaimers and ethical guidelines that apply to the journal pertain. ACS cannot be held responsible for errors or consequences arising from the use of information contained in these “Just Accepted” manuscripts.

1  
2  
3  
4  
5  
6  
7  
8  
9  
10  
11  
12  
13  
14  
15  
16  
17  
18  
19  
20  
21  
22  
23  
24  
25  
26  
27  
28  
29  
30  
31  
32  
33  
34  
35  
36  
37  
38  
39  
40  
41  
42  
43  
44  
45  
46  
47  
48  
49  
50  
51  
52  
53  
54  
55  
56  
57  
58  
59  
60

# Exploiting the 4-Phenylquinazoline Scaffold for the Development of High Affinity Fluorescent Probes for the Translocator Protein (TSPO)

*Ciro Milite,<sup>†,‡</sup> Elisabetta Barresi,<sup>‡,§</sup> Eleonora Da Pozzo,<sup>‡</sup> Barbara Costa,<sup>‡</sup> Monica Viviano,<sup>†</sup>  
Amalia Porta,<sup>†</sup> Anna Messere,<sup>Δ</sup> Gianluca Sbardella,<sup>†</sup> Federico Da Settimo,<sup>‡</sup> Ettore Novellino,<sup>§</sup>  
Sandro Cosconati,<sup>Δ,\*</sup> Sabrina Castellano,<sup>†,¶\*</sup> Sabrina Taliani,<sup>‡,\*</sup> Claudia Martini.<sup>‡</sup>*

<sup>‡</sup>Dipartimento di Farmacia, Università di Pisa, Via Bonanno 6, 56126 Pisa, Italy. <sup>†</sup>Dipartimento di Farmacia, Università di Salerno, Via Giovanni Paolo II 132, 84084 Fisciano, Salerno, Italy.

<sup>¶</sup>Dipartimento di Medicina, Chirurgia e Odontoiatria "Scuola Medica Salernitana", Università di Salerno, Via Salvador Allende, Baronissi, I-84081 Salerno, Italy. <sup>§</sup>Dipartimento di Farmacia, Università di Napoli "Federico II", Via D. Montesano 49, 80131 Napoli, Italy. <sup>Δ</sup>DiSTABiF, University of Campania Luigi Vanvitelli, 81100 Caserta, Italy.

## Abstract

The quinazoline class was exploited to search for a new Translocator Protein (TSPO) fluorescent probe endowed with improved affinity and Residence Time (RT). Computational studies on an “in-house” collection of quinazoline derivatives, featuring highly steric demanding groups at the amide nitrogen, suggested that, despite their molecular extension, these ligands are still easily lodged in the TSPO binding site. Binding assays supported this hypothesis, highlighting a low nanomolar/subnanomolar affinity of these ligands, together with a higher RT of the representative compound **11** with respect to our previously reported indole-based fluorescent probe. Thanks to the amenability of the amide nitrogen atom to be substituted with bulky groups, we developed quinazoline-based imaging tools by fluorescently labeling the scaffold at this position. Probes with relevant TSPO affinity, favorable spectroscopic properties, and improved RT were identified. Results from fluorescence microscopy showed that these probes specifically labeled the TSPO at mitochondrial level in U343 cell line.

## Introduction

Neuroinflammation and activation of glial cells are important pathological processes that are involved in the progression of many neurological disorders, including multiple sclerosis, amyotrophic lateral sclerosis, Parkinson’s disease, Huntington’s disease, Alzheimer’s disease, and stroke. In particular, the activation of microglial cells involves changes in their morphology and acquisition of new functions, including the expression and release of diverse proinflammatory molecules and the phagocytosis of dead cells.<sup>1</sup>

During the past decade, several studies have validated the Translocator Protein 18 kDa (TSPO) as a biomarker of neuroinflammation as well as of brain injury.<sup>2-4</sup> This is a highly conserved protein throughout evolution, from bacteria to humans, mainly located on the outer mitochondrial membrane of steroid-producing tissues (testis, adrenal cortical, ovarian granulose, and luteal cells)

1  
2  
3 and it has been proposed to be an important player in the transport of cholesterol into mitochondria,  
4  
5 the first and rate-limiting step for steroid hormone synthesis.<sup>5</sup> Furthermore, considerable evidence  
6  
7 supports its regulatory role in a number of other cellular processes, including apoptosis, cell  
8  
9 proliferation, cellular respiration and immunomodulation.<sup>6</sup>  
10

11  
12 Recently, a controversy surrounding the exact physiological role of this protein<sup>7</sup> emerged  
13  
14 following reports proposing its catalytic activity,<sup>8</sup> as well as challenging its essentiality for  
15  
16 steroidogenesis.<sup>9-11</sup> Nevertheless, the reproducibly high level of expression in areas of inflammation  
17  
18 in the brain still validate TSPO as a sensitive imaging biomarker to evaluate neuroinflammation.<sup>4</sup>  
19  
20 Indeed, in the central nervous system (CNS), the expression level of TSPO is low in healthy brains,  
21  
22 but the protein is overexpressed in activated glial cells following CNS pathological conditions,  
23  
24 including gliomas, multiple sclerosis, as well as Alzheimer's disease.<sup>2,4,12</sup>  
25  
26

27  
28 Since its identification by means of the benzodiazepines diazepam and 4'-chlorodiazepam (Ro5-  
29  
30 4864),<sup>13</sup> a number of high affinity and selectivity TSPO ligands have been developed from different  
31  
32 structural classes, including isoquinoline carboxamides (e.g., 1-(2-chlorophenyl)-*N*-methyl-*N*-(1-  
33  
34 methylpropyl)-1-isoquinolinecarboxamide (PK11195, **1**, Chart 1) widely considered as a  
35  
36 prototypical TSPO ligand and used as a reference compound in biological experiments),<sup>14</sup>  
37  
38 aryloxyanilides (e.g., *N*-(2,5-dimethoxybenzyl)-*N*-(5-fluoro-2-phenoxyphenyl)acetamide  
39  
40 (DAA1106) and *N*-acetyl-*N*-(2-methoxybenzyl)-2-phenoxy-5-pyridinamine (PBR28)),<sup>15,16</sup> 2-  
41  
42 phenyl-imidazo[1,2-*a*]pyridine acetamides (e.g., alpidem).<sup>17</sup> Many of these ligands have been  
43  
44 developed to visualize activated microglia via several imaging techniques.<sup>18</sup>  
45  
46

47  
48 In this context, we recently reported two class of highly potent and selective TSPO ligands, the 2-  
49  
50 arylindol-3-glyoxylamides **A**<sup>19-22</sup> and the 4-phenylquinazoline-2-carboxamides **B**, designed as  
51  
52 azaisosteres of **1** (Chart 1).<sup>23,24</sup> Ligands from class **A** were developed to fluorescent probes (see  
53  
54 compound **2** as an example, Chart 1) useful for investigating the localization and the expression  
55  
56 level of TSPO,<sup>25,26</sup> and to a novel positron emission tomography (PET) radioligand labeled with  
57  
58 carbon-11 (**3**, Chart 1) able to enter monkey's brain and give a high proportion of TSPO-specific  
59  
60

binding.<sup>27</sup> Similarly, ligands from 4-phenylquinazoline-2-carboxamide class have been developed to visualize activated microglia via PET; a useful radioligand (**4**, Chart 1), the direct 4-azaisostere of **1**, was identified and demonstrated to possess an array of properties that are superior to those reported for [<sup>11</sup>C]-**1**, including higher affinity, lower lipophilicity, higher TSPO-specific signal, and, most importantly, very low genotype sensitivity *in vitro*.<sup>28</sup> On these premises, compound **4** was further evaluated for its *in vivo* sensitivity in the brain and peripheral organs in human subjects, showing adequate sensitivity to robustly image all three affinity genotypes in the human brain.<sup>29</sup> Taken together, all these findings corroborate the worth of the 4-phenylquinazoline-2-carboxamide chemotype in the development of specific TSPO ligands, as well as molecular probes suitable for TSPO imaging.

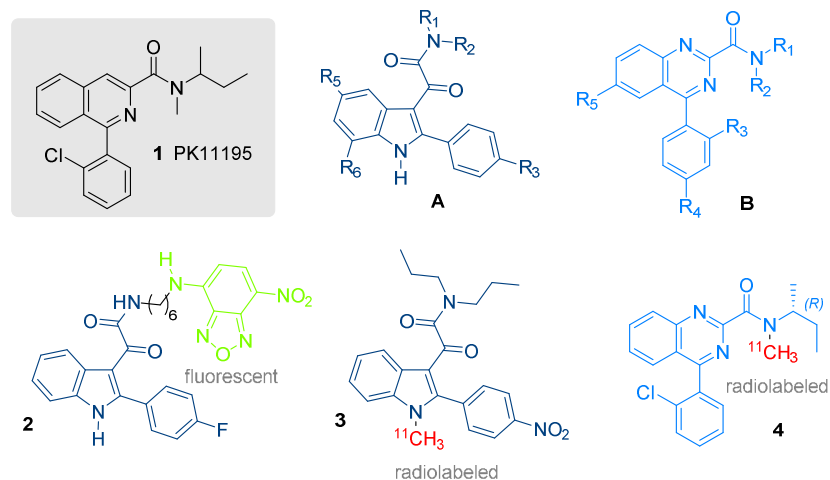


**Chart 1.** General structure of 2-arylindol-3-glyoxylamides (**A**)<sup>19-21</sup> and 4-phenylquinazoline-2-carboxamides (**B**),<sup>23,24</sup> together with **1** and fluorescent (**2**)<sup>25,26</sup> and radiolabeled (**3**, **4**)<sup>27-29</sup> probes belonging from classes **A** and **B**.

In the present study, we evaluated the feasibility of developing novel fluorescently labeled TSPO ligands with high specificity and attractive spectroscopic properties, featuring the 4-phenylquinazoline-2-carboxamide scaffold. In this respect, ligands incorporating fluorescent probes may represent a safer, faster, and less expensive tool to achieve TSPO imaging if compared to the classic radiolabeled ligand. In general, a fluorescent ligand can be rationally designed to retain the pharmacological profile of the parent unlabeled ligand, thus allowing for the localization and real-

1  
2  
3 time monitoring of processes triggered by ligand-receptor interactions (i.e internalization,  
4 trafficking, sequestration, and recycling) within a living cell. In addition, the displacement of  
5 fluorescent probes from their binding sites of a target protein by non-fluorescent ligands allows for  
6  
7 the identification of the sites recognized by the ligands.<sup>30</sup>  
8  
9  
10

## 11 12 13 14 **Results and discussion**

### 15 16 **Basis of the project.**

17  
18 The starting point for the probe development was our previously published two-dimensional (2D)  
19 pharmacophore/topological model,<sup>24</sup> according to which the *N*-benzyl-*N*-ethyl-disubstituted  
20 quinazolines **5-6** (Chart 2 and Figure 1A)<sup>24</sup> place their *N*-benzyl substituent towards the external  
21 part of the receptor, herein referred to as L4 (see compound **6** as an example in Figure 1A). In  
22 principle, this would outline that the aforementioned group could be functionalized with a steric  
23 demanding fluorescent tracer without affecting the binding affinity for the target TSPO.  
24  
25  
26  
27  
28  
29  
30

31  
32 In this respect, the availability of an “in-house” library of quinazoline compounds encouraged us  
33 to pursue derivatives of compounds **5** and **6** for the development of our probe. Considering the  
34 elevated costs connected with the radioligand binding experiments, rather than directly screening all  
35 of them, a fast, and cost-effective, *in silico* pre-evaluation was firstly performed. Therefore, a three-  
36 dimensional (3D) model of interaction between the rTSPO and a selection of quinazoline  
37 derivatives (compounds **7-14**), featuring highly steric demanding groups at the amide nitrogen (see  
38 Chart 2 and Figure 1B) was generated. In particular, compounds **7-12** present a single bulky  
39 substituent on amide nitrogen, whereas compounds **13** and **14** were characterized by double  
40 substitution with steric demanding groups.  
41  
42  
43  
44  
45  
46  
47  
48  
49  
50

51  
52 According to these calculations, all the selected compounds would interact within the TSPO  
53 binding cleft by placing the *p*-substituted-benzyl group in the wide L4 cleft; differently from what  
54 happens for compounds **5** and **6**, now the 4-phenyl substituent is lodged in the L1 cleft, while the  
55 quinazoline core resides in the L3 one. Nevertheless, when analyzing the scores calculated by Glide  
56  
57  
58  
59  
60

docking software, the inspected compounds (**6** and **7-12**) are predicted to have a similar affinity for the TSPO. On the other hand, Glide was not able to dock **13** and **14** in the TSPO site most probably due to the steric hindrance of the double substitution at the amide nitrogen.

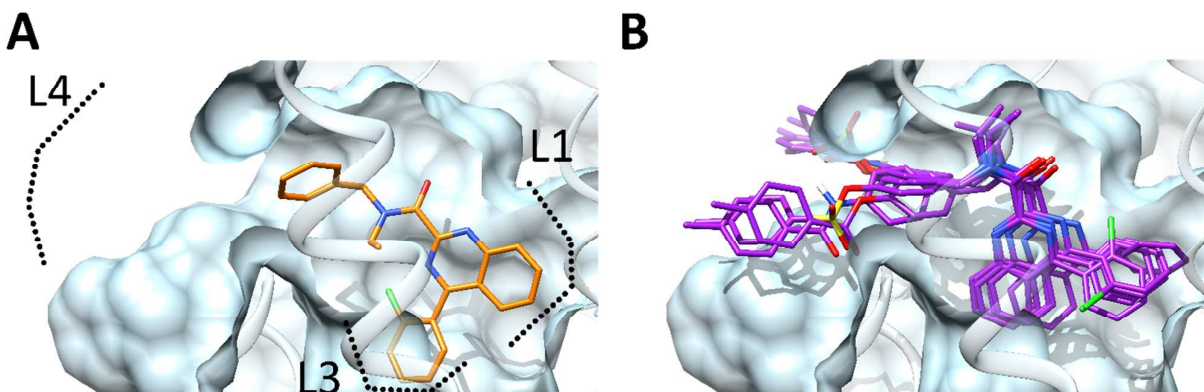
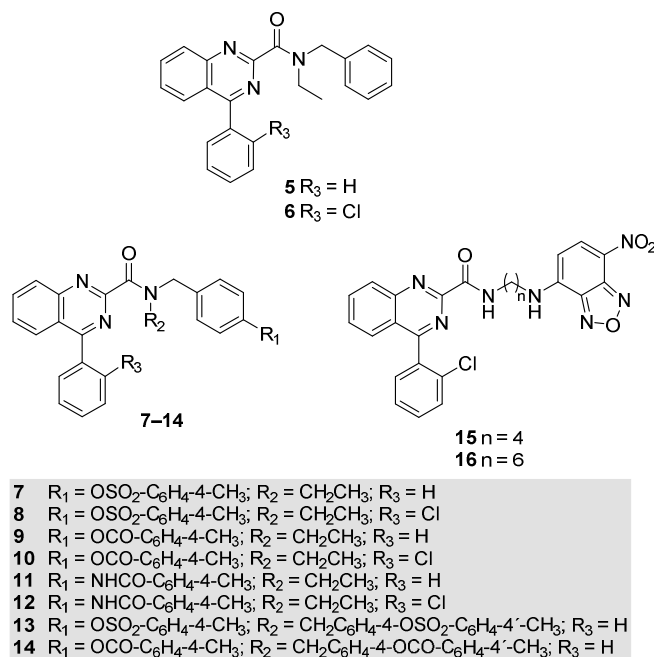


**Figure 1.** Binding mode of compound **6** (panel A, orange sticks) and **7-12** (panel B, purple sticks) into the rTSPO binding site (cyan ribbons and surface). In panel (A) the three receptor clefts identified from the topological model are also outlined.

Encouraged by molecular modeling results, the affinity of the 4-phenylquinazoline compounds **7-14** at the TSPO was determined by binding competition experiments against [ $^3\text{H}$ ]-**1**, performed on rat kidney mitochondrial membranes (Table 1). As predicted by computational studies, all the compounds show high affinity for TSPO in the nanomolar/subnanomolar range, the only exception being compounds **13** and **14**, which feature two bulky substituents at the amide nitrogen, substantiating our work hypothesis. In term of structure-affinity relationships, the insertion at the benzyl *para*-position of a highly steric demanding group such as *p*-toluensulfonyloxy (**7**, **8**), *p*-toluencarbonyloxy (**9**, **10**), *p*-toluencarbonylamino (**11**, **12**) is well tolerated in terms of TSPO binding affinity since all derivatives show low nanomolar/subnanomolar  $K_i$  values. The cooperative effect of the chlorine at 2'-position of the 4-phenyl ring seemed necessary for subnanomolar affinity only when  $R_1$  is a *p*-toluencarbonyloxy or *p*-toluencarbonylamino group.

Reaching a high binding affinity for the biological target is not the only demand to develop efficient pharmacological tools and drugs. In fact, emerging evidence is demonstrating that one of the key factors characterizing the binding performances of a ligand is the Residence Time (RT),

which is the time for which the ligand interacts with its target.<sup>31</sup> In this respect, a kinetic radioligand binding assay was recently set up to determine the RT of ligands in their interaction with TSPO by using a theoretical mathematical model successfully applied to other ligand-target systems.<sup>32-35</sup> In principle, this kinetic parameter could represent a crucial key requirement for the suitability of a novel fluorescent probe, as it is reasonable to speculate that a relatively high RT may be advantageous for imaging studies. Thus, experiments were performed to measure the  $K_{on}$  and  $K_{off}$  rate constants of our previously published indole-based fluorescent probe **2**, together with that of the highest affinity compound **8**; then, RTs for **2** and **8** were derived from the values of the corresponding  $K_{off}$  and compared with that of **1**<sup>32</sup> (Table 2). Results of these inspections demonstrated that **2** and **1** are rapid dissociating competitors of the [<sup>3</sup>H]-**1** binding site, with RT values of  $36 \pm 2$  min and  $34 \pm 3$  min, respectively. In contrast, derivative **8** shows a longer value (RT =  $55 \pm 4$  min), prompting us to develop a fluorescent phenylquinazoline-based fluorescent probe with improved RT.

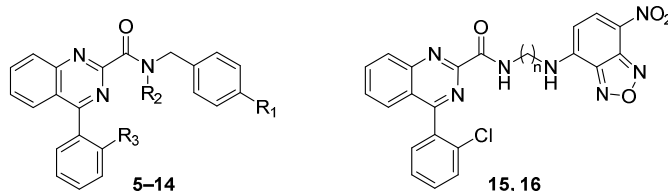


**Chart 2.** General structure of 4-phenylquinazoline TSPO ligands (**5-14**) and fluorescent probes (**15, 16**).

### Design of 4-phenylquinazoline-based fluorescent probes, TSPO Affinity and Kinetic Assays.

The inspection of the molecular alignment shown in Figure 1B, the high nanomolar/subnanomolar TSPO affinity of the bulky phenylquinazoline ligands (Table 1), along with the RT value of compound **8** strongly supported the design of fluorescent probes from this chemotype, by inserting the fluorogenic 7-nitro-2,1,3-benzoxadiazol-4-yl (NBD) moiety at the 4-phenylquinazoline-2-carboxylic acid through an alkylenediamine spacer (tetramethylene, n=4, and hexamethylene, n=6, diamino spacer for compounds **15** and **16**, respectively, Chart 2). The length of the spacer alkyl chain was modified to introduce some flexibility that would favor self-adaptation of the ligands into the L4 pocket of the receptor binding site, so as to maintain high TSPO affinity. The well-known NBD group was selected as the fluorophore because its small size does not generally affect the affinity of the parent ligand for the target protein. Furthermore, NBD is solvatochromic, in that it exhibits low fluorescent activity in polar and protic environments but becomes highly fluorescent in nonpolar solvents or when bound to membranes or to hydrophobic clefts such as protein pockets.<sup>36</sup> These properties suggest that an NBD fluorescent tracer may possess reduced background fluorescence from nonbound fluorescent tracer allowing for both homogeneous detection and use in imaging applications.

As reported in Table 1, the fluorescent probes **15** and **16** showed significant TSPO affinity, with comparable  $K_i$  values in the nanomolar range, suggesting that the two linkers (4 or 6 methylene units, **15** and **16**, respectively) are equally effective for a successful accommodation of the molecule in the receptor L4 cleft of the TSPO binding site.

**Table 1.** TSPO Binding Affinity of Quinazoline Derivatives **5-16**.

cmpd	R <sub>1</sub>	R <sub>2</sub>	R <sub>3</sub>	n	I% (1 μM) or K <sub>i</sub> (nM) <sup>a</sup>
<b>5<sup>b</sup></b>	H	CH <sub>2</sub> CH <sub>3</sub>	H	-	1.1 ± 0.1
<b>6<sup>b</sup></b>	H	CH <sub>2</sub> CH <sub>3</sub>	Cl	-	0.23 ± 0.02
<b>7</b>	OSO <sub>2</sub> -C <sub>6</sub> H <sub>4</sub> -4-CH <sub>3</sub>	CH <sub>2</sub> CH <sub>3</sub>	H	-	0.51 ± 0.05
<b>8</b>	OSO <sub>2</sub> -C <sub>6</sub> H <sub>4</sub> -4-CH <sub>3</sub>	CH <sub>2</sub> CH <sub>3</sub>	Cl	-	0.47 ± 0.05
<b>9</b>	OCO-C <sub>6</sub> H <sub>4</sub> -4-CH <sub>3</sub>	CH <sub>2</sub> CH <sub>3</sub>	H	-	3.5 ± 0.4
<b>10</b>	OCO-C <sub>6</sub> H <sub>4</sub> -4-CH <sub>3</sub>	CH <sub>2</sub> CH <sub>3</sub>	Cl	-	0.50 ± 0.05
<b>11</b>	NHCO-C <sub>6</sub> H <sub>4</sub> -4-CH <sub>3</sub>	CH <sub>2</sub> CH <sub>3</sub>	H	-	3.5 ± 0.4
<b>12</b>	NHCO-C <sub>6</sub> H <sub>4</sub> -4-CH <sub>3</sub>	CH <sub>2</sub> CH <sub>3</sub>	Cl	-	0.61 ± 0.05
<b>13</b>	OSO <sub>2</sub> -C <sub>6</sub> H <sub>4</sub> -4-CH <sub>3</sub>	CH <sub>2</sub> C <sub>6</sub> H <sub>4</sub> -4-OOSO <sub>2</sub> -C <sub>6</sub> H <sub>4</sub> -4-CH <sub>3</sub>	H	-	23.5 ± 2.5%
<b>14</b>	OCO-C <sub>6</sub> H <sub>4</sub> -4-CH <sub>3</sub>	CH <sub>2</sub> C <sub>6</sub> H <sub>4</sub> -4-OCO-C <sub>6</sub> H <sub>4</sub> -4'-CH <sub>3</sub>	H	-	40.5 ± 2.0%
<b>15</b>	-	-	-	4	19.2 ± 2.9
<b>16</b>	-	-	-	6	25.3 ± 4.0
<b>1</b>	-	-	-	-	3.39 ± 0.34 <sup>c</sup>

<sup>a</sup>The concentration of test molecules that inhibited [<sup>3</sup>H]-**1** binding to rat kidney mitochondrial membranes by 50% (IC<sub>50</sub>) was determined with six concentrations of the compounds, each performed in triplicate. K<sub>i</sub> values and inhibition percentages at 1 μM are the mean ± SEM of three determinations. <sup>b</sup>Data taken from ref. 25. <sup>c</sup>Data taken from ref. 32.

Compound **15** was selected as representative and evaluated in competition kinetic association assays, revealing K<sub>on</sub> = 7.10 ± 2.00 × 10<sup>5</sup> M<sup>-1</sup> min<sup>-1</sup>, and K<sub>off</sub> = 0.019 ± 0.005 min<sup>-1</sup> (Table 2). The RT was calculated to be 53 ± 7 min (Table 2), which is comparable to that of **8**. Since **15** is a slower dissociation competitor than both fluorescent indole-based probe **2** and **1**, this ligand was used for further evaluation in experiments aimed at labeling TSPO in U343 glioma cells.

**Table 2.** TSPO binding affinity and kinetic parameters of compounds **1**, **2**, **10**, and **17**.

TSPO ligand	Equilibrium $K_i$ (nM)	$K_{on}$ ( $M^{-1}, min^{-1}$ )	$K_{off}$ ( $min^{-1}$ )	$RT = 1/K_{off}$ (min)
<b>2</b>	$12.1 \pm 1.0^a$	$2.09 \pm 0.28 \times 10^6$	$0.028 \pm 0.001$	$36 \pm 2$
<b>8</b>	$0.51 \pm 0.05$	$6.23 \pm 0.56 \times 10^7$	$0.018 \pm 0.001$	$55 \pm 4$
<b>15</b>	$19.2 \pm 2.9$	$7.10 \pm 2.00 \times 10^5$	$0.019 \pm 0.005$	$53 \pm 7$
<b>1</b>	$3.39 \pm 0.34^b$	$9.30 \pm 0.94 \times 10^{6b}$	$0.029 \pm 0.003^b$	$34 \pm 3^b$

$K_i$  were obtained from [ $^3H$ ]-**1** competition binding experiments at equilibrium.  $K_{on}$  and  $K_{off}$  values were obtained from competitive association kinetics assays using [ $^3H$ ]-**1** as a probe. Values are means  $\pm$  SEM of three independent experiments, each performed in duplicate. <sup>a</sup>Data taken from ref. 25; <sup>b</sup>Data taken from ref. 32.

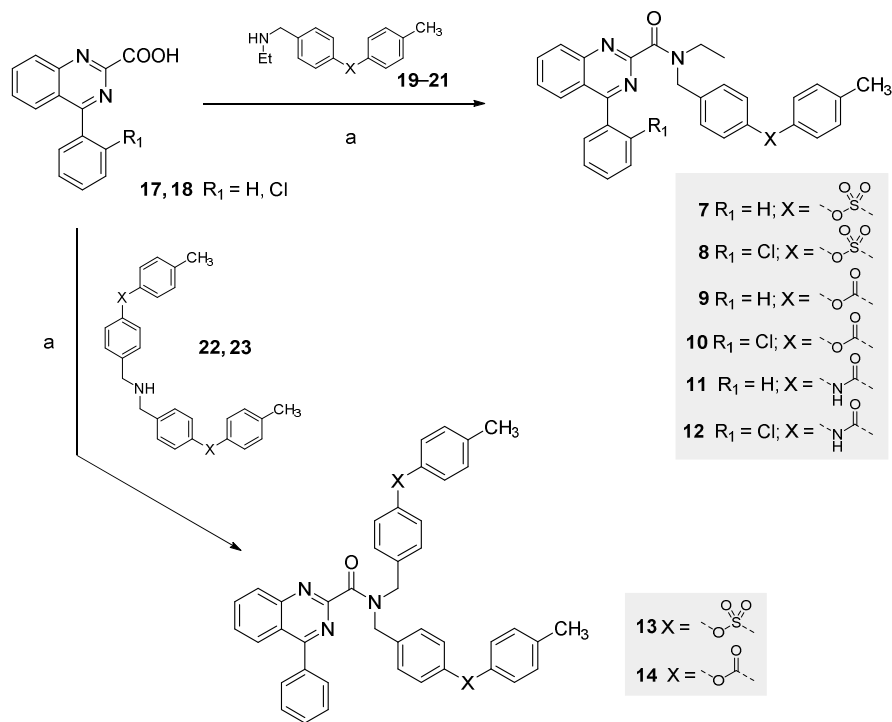
## Chemistry

The synthetic protocols for the preparation of compounds **7-14** are outlined in Scheme 1.

Carboxylic acids **17** and **18**, key intermediates in the synthesis of target compounds **7-14**, were prepared by condensation of 2-aminobenzophenone or 2-amino-2'-chloro-benzophenone with glyoxylic acid in the presence of ammonium acetate, followed by light irradiation with 20 W halogen tungsten lamp, as previously reported.<sup>23,24</sup>

Compounds **7-14** were obtained by direct coupling reaction of acids **17** and **18** and the appropriate secondary amines **19-23**, by carboxylate activation with using hydroxybenzotriazole (HOBT) and O-benzotriazole-*N,N,N',N'*-tetramethyl-uronium-hexafluoro-phosphate (HBTU) in the presence of Hünig's base (*N,N*-diisopropylethylamine, DIEA) in dry THF-DMF.

## Scheme 1

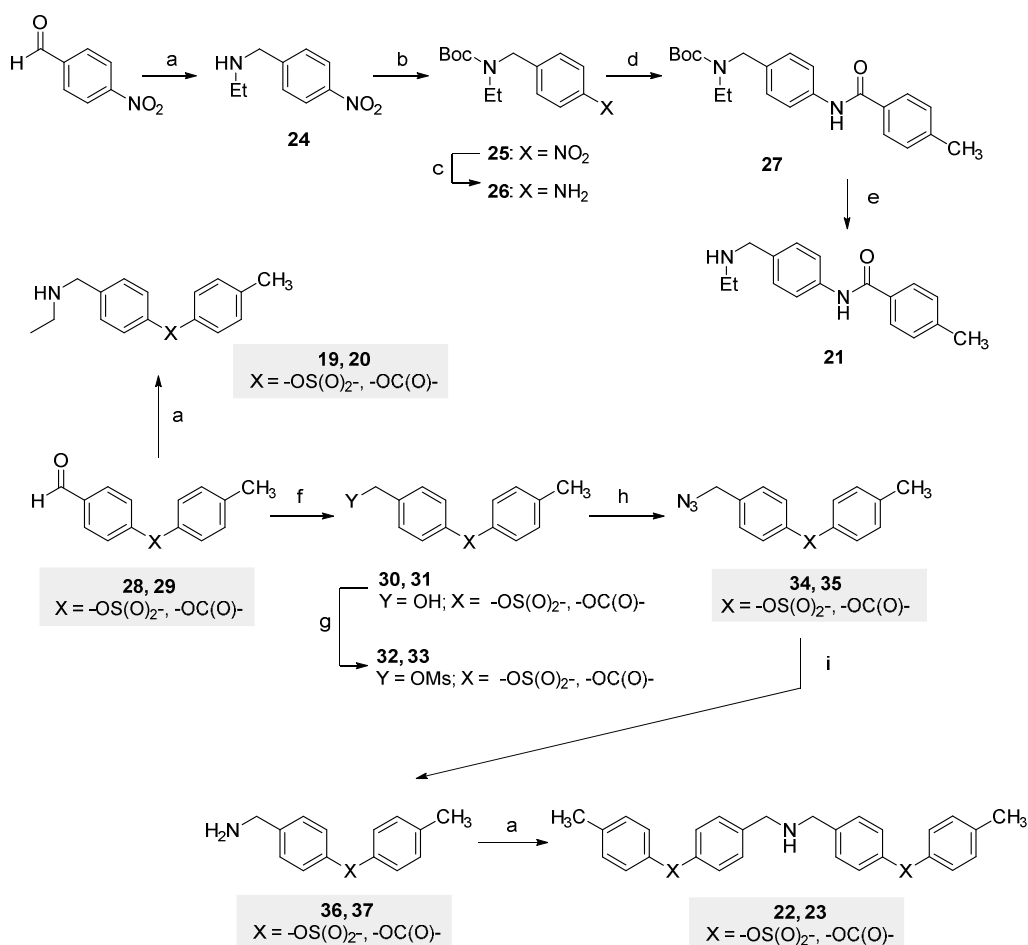


**Reagents and conditions:** (a) DIEA, HOBt, HBTU, THF/DMF 7:2, room temperature, overnight, 58–85%.

Secondary amines **19** and **20** were promptly prepared by reductive alkylation of the appropriate aldehyde (**28** and **29**, respectively) with ethylamine using sodium borohydride ( $\text{NaBH}_4$ ) in EtOH. Conversely, the preparation of amines **21–23** was not immediate even if straightforward (Scheme 2).

Reductive alkylation of nitrobenzaldehyde with ethylamine furnished the *N*-(4-nitrobenzyl)ethanamine **24** which, after classical Boc protection (compound **25**), was reduced with zinc powder in acetic acid to give the corresponding amino derivative **26**. Subsequent coupling with 4-methylbenzoic acid, using HOBt and HBTU in the presence of DIEA, furnished amide **27**, which, after Boc deprotection with TFA in dry  $\text{CH}_2\text{Cl}_2$ , provided the desired secondary amine **21**.

## Scheme 2



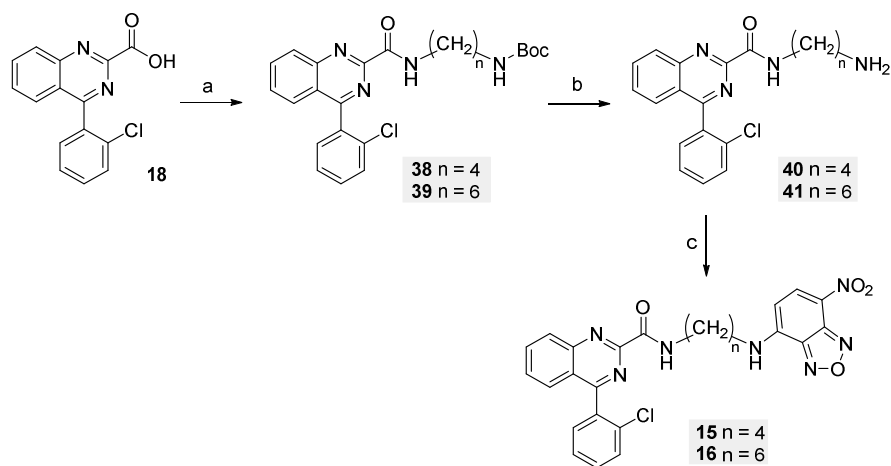
**Reagents and conditions:** (a) ethylamine, EtOH, room temperature, 12 h, then NaBH<sub>4</sub>, 0 °C, 71–97%; (b) Boc<sub>2</sub>O, EtOAc, room temperature, 1 h, 92%; (c) Zn, AcOH, room temperature, 10 min, 90%; (d) 4-methylbenzoic acid, DIEA, HOBt, HBTU, THF/DMF 7:2, room temperature, overnight, 72%; (e) TFA/CH<sub>2</sub>Cl<sub>2</sub> 3:7, room temperature, 30 min, 99%; (f) NaBH<sub>4</sub>, MeOH, 0 °C, 93–94%; (g) MsCl, TEA, CH<sub>2</sub>Cl<sub>2</sub>, 0 °C, 45 min; (h) NaN<sub>3</sub>, DMF, 80 °C, 1 h, 88–91%; (i) H-Cube Pro™, full-H<sub>2</sub> mode, 30 °C, 10 bar, 1 mL min<sup>-1</sup> flow rate. 10% Pd/C CatCart cartridge, MeOH, 90–96%.

The preparation of secondary amines **22** and **23** started with the reduction of 4-(4-toluenesulfonyloxy)benzaldehyde **28** and 4-(4-methylbenzoyloxy)benzaldehyde **29**, to the corresponding alcohols **30** and **31**, respectively. The transformation of the latter into amines **36** and **37** was performed by mesylation (compound **32** and **33**), subsequent substitution reaction with sodium azide (compound **34** and **35**), and reduction by means of a continuous-flow hydrogenation protocol employing a fixed-bed catalyst (H-Cube Pro™, Thales Nanotechnology Inc.) and using

catalyst cartridges filled with 10% Pd/C. Finally, reductive alkylation with benzaldehydes **28** and **29** furnished the desired secondary amines **22** and **23**.

The general synthetic pathway yielding the novel phenylquinazoline-2-carboxamides **15** and **16** in the best yields is outlined in Scheme 3. After activation with thionyl chloride, the carboxylic acid **18** was coupled with *N*-Boc-1,4-butanediamine or *N*-Boc-1,6-hexanediamine in the presence of TEA at room temperature to yield derivatives **38** and **39**, respectively. Boc deprotection with TFA in dry CH<sub>2</sub>Cl<sub>2</sub> gave the corresponding amine **40** and **41**, which were then reacted with the fluorescent 4-chloro-7-nitrobenzofurazan in dry DMF, at room temperature and in the presence of TEA, yielding the desired fluorescent compounds **15** and **16**.

**Scheme 3.**



**Reagents and conditions:** (a) SOCl<sub>2</sub>, reflux, 2 h, then *N*-Boc-1,4-butanediamine or *N*-Boc-1,6-hexanediamine, TEA, THF, room temperature, 48 h, 70–71%; (b) TFA/CH<sub>2</sub>Cl<sub>2</sub> 1:2, room temperature, 3 h, 74–86%; (c) 4-chloro-7-nitrobenzofurazan, DMF, TEA, room temperature, overnight, 55–72%.

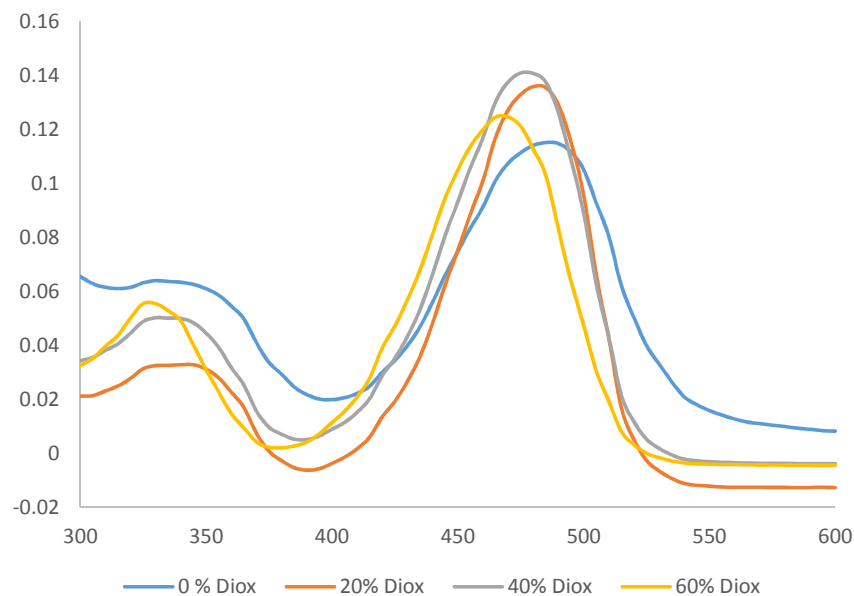
### Spectroscopic Properties of Fluorescent Ligand **15**

The ultraviolet absorption and the emission spectra of compound **15** were measured to investigate the spectroscopic properties of the ligand and how these were affected by the environment.

Compound **15**, dissolved in dimethyl sulfoxide (DMSO), was diluted to a final concentration of 10

1  
2  
3  $\mu\text{M}$  in different assay solutions (from aqueous to 60% v/v dioxane-water phosphate buffered saline  
4 (PBS)). The percentage of DMSO did not exceed 1% of the final assay volume solution.  
5  
6

7 Figure 2 shows the absorption spectra of compound **15**. In an aqueous solution, the absorption  
8 spectra of compound **15** is characterized by two absorption maxima at 335 nm and 485 nm with  
9 extinction coefficients of  $\epsilon = 5118 \text{ M}^{-1} \text{ cm}^{-1}$  and  $\epsilon = 9210 \text{ M}^{-1} \text{ cm}^{-1}$ , respectively.  
10  
11  
12  
13

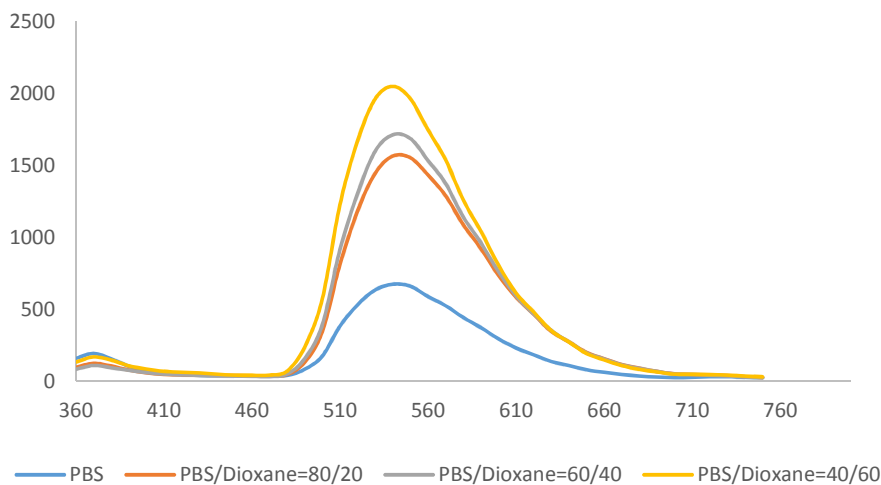


14  
15  
16  
17  
18  
19  
20  
21  
22  
23  
24  
25  
26  
27  
28  
29  
30  
31  
32  
33  
34  
35 **Figure 2.** Absorption spectra of compound **15** at 10  $\mu\text{M}$  in solutions varying from aqueous to 60%  
36 dioxane-water (v/v) PBS.  
37  
38

39  
40 When **15** was dissolved in PBS solution containing 20% of dioxane, the wavelengths of the  
41 absorption maxima remained almost constant, but the spectrum was characterized by an increase in  
42 the extinction coefficients and a small hypsochromic shift of the 485 nm band. A further increase in  
43 the extinction coefficients and a small hypsochromic shift of the 485 nm band. A further increase in  
44 hydrophobicity of the medium (40% dioxane water (v/v) PBS) caused a slight increase in the  
45 extinction coefficients. A decrease in the extinction coefficients was obtained further increasing the  
46 hydrophobicity of the medium (60% dioxane water (v/v) PBS), even if these values remained  
47 higher with respect to those observed in aqueous solution.  
48  
49  
50  
51  
52  
53  
54

55  
56 Figure 3 shows the emission spectra of compound **15**. As expected, the decrease in polarity of the  
57 environment (from the aqueous buffer to 60% dioxane in PBS) induced an approximately 3-fold  
58 environment (from the aqueous buffer to 60% dioxane in PBS) induced an approximately 3-fold  
59  
60

1  
2  
3 increase in quantum yield. This phenomenon was accompanied by a slight blue-shift of the  
4  
5 emission maximum from 542 to 538 nm.  
6



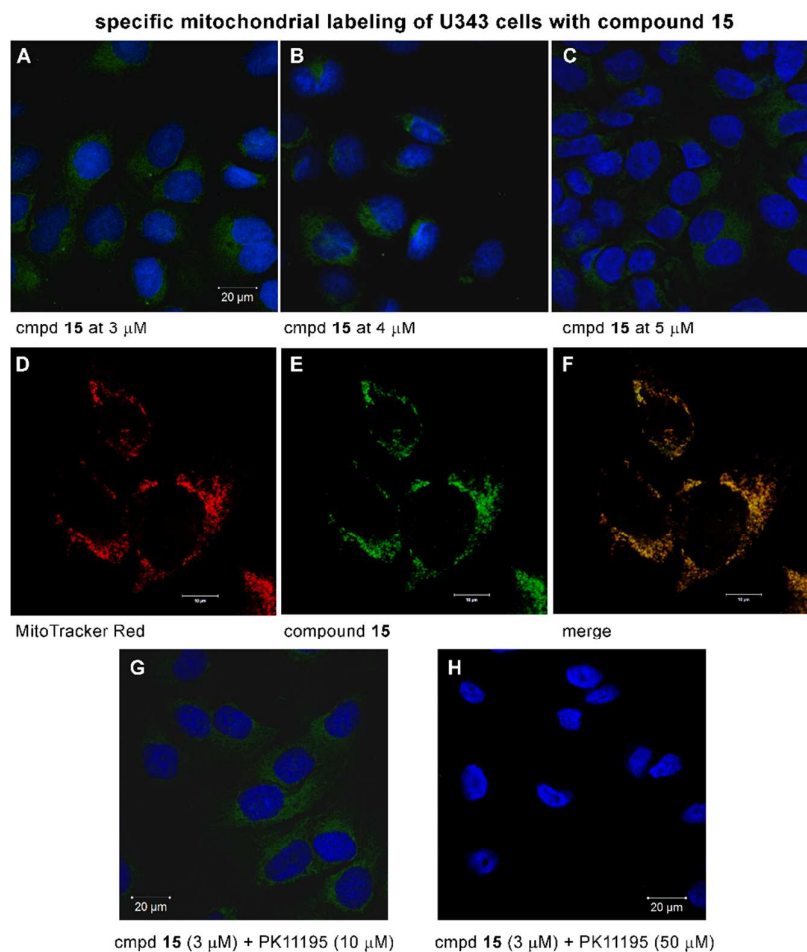
33  
34  
35  
36  
37  
38  
39  
40  
41  
42  
43  
44  
45  
46  
47  
48  
49  
50  
51  
52  
53  
54  
55  
56  
57  
58  
59  
60

**Figure 3.** The influence of the polarity of the medium on the fluorescence of compound **15** was investigated by the addition of dioxane (indicated in % v/v) in PBS measured at a  $\lambda_{\text{max}}$  of 470 nm.

### Fluorescent labeling of human glioblastoma cell line U343

Compounds **15** and **16** were then evaluated for their ability to specifically label TSPO in human glioblastoma cell line U343. Representative confocal images in Figure 4 demonstrate uniform cytoplasm labeling of cells with a granular structure resembling a mitochondrial expression pattern. Labeling was clearly detected using compound **15** at 3  $\mu\text{M}$  (Figure 4A) and no significant difference was observed with higher ligand concentrations (Figure 4B). Similar results were obtained with **16** (data not shown).

Specific mitochondrial labeling was confirmed by the co-localization of our TSPO affinity probes with the mitochondrion-specific probe MitoTracker Red. As shown in Figure 4C–E, merged images revealed a clearly overlap between the MitoTracker Red signal and the green one of compound **15**. Similar results were obtained with **16** (data not shown).



34  
35  
36  
37  
38  
39  
40  
41  
42

**Figure 4.** Compound **15** specifically labels mitochondria of human glioblastoma cell line U343. Panels A–C: U343 cells stained with **15** (3, 4 and 5  $\mu\text{M}$ ); panels D–F: comparison of U343 cells stained with mitochondria specific dye MitoTracker Red (D) and with compound **15** (E) and merged image (F); panels G, H: human glioblastoma cell line U343 stained with **15** (3  $\mu\text{M}$ ) in the presence of **1** (10 and 50  $\mu\text{M}$ , respectively).

43  
44  
45  
46  
47  
48  
49  
50  
51

Moreover, displacement assays using the non-fluorescent ligand **1** (Figure 4G, and H) indicate that the tested compounds specifically label TSPO. The fluorescent staining obtained using 3  $\mu\text{M}$  **15** was displaced when **1** was used at concentrations higher than 10  $\mu\text{M}$  and the complete displacement staining was achieved using 50  $\mu\text{M}$  **1**.

52  
53  
54  
55

Under this experimental conditions, **15** and **16** did not show significant cytotoxic activity, as determined by MTT method (see Figure S1 in Supporting Information).

## 56 57 58 59 60

### Conclusion

1  
2  
3 Molecular modeling studies and results from a biological evaluation of a small “in-house”  
4 collection of bulky phenylquinazoline ligands strongly supported the design of fluorescent probes  
5 from this chemotype. The fluorogenic 7-nitro-2,1,3-benzoxadiazol-4-yl (NBD) moiety was then  
6 inserted at the 4-phenylquinazoline-2-carboxylic acid through an alkylenediamine spacer yielding  
7 novel fluorescently tagged TSPO ligands endowed with high affinity, attractive spectroscopic  
8 properties and improved RT with respect to our previously developed fluorescent indole-based  
9 probe. Finally, results from fluorescence microscopy showed that these probes specifically label the  
10 TSPO at the mitochondrial level U343 glioma cells, thereby representing potential new imaging  
11 biomarkers for this protein.  
12  
13  
14  
15  
16  
17  
18  
19  
20  
21

## 22 23 24 25 **Experimental Section**

26  
27 **Chemistry.** All chemicals were purchased from Sigma-Aldrich (Milan, Italy) or Fluorochem Ltd  
28 (Hadfield, United Kingdom) and were of the highest purity. All solvents were reagent grade and,  
29 when necessary, were purified and dried by standard methods. All reactions requiring anhydrous  
30 conditions were conducted under a positive atmosphere of nitrogen in oven-dried glassware.  
31 Standard syringe techniques were used for anhydrous addition of liquids. Reactions were routinely  
32 monitored by TLC performed on aluminum-backed silica gel plates (Merck DC, Alufolien  
33 Kieselgel 60 F254) with spots visualized by UV light ( $\lambda = 254, 365$  nm) or using a  $\text{KMnO}_4$  alkaline  
34 solution. Solvents were removed using a rotary evaporator operating at a reduced pressure of  $\sim 10$   
35 Torr. Organic solutions were dried over anhydrous  $\text{Na}_2\text{SO}_4$ . Chromatographic separations were  
36 performed on silica gel (silica gel 60, 0.015–0.040 mm; Merck DC) columns. Melting points were  
37 determined on a Stuart SMP30 melting point apparatus in open capillary tubes and are uncorrected.  
38  
39  $^1\text{H}$  and  $^{13}\text{C}$  NMR spectra were recorded at 400 and 100 MHz respectively on a Bruker Ascend™  
40 400 spectrometer. Chemical shifts are reported in  $\delta$  (ppm) relative to the internal reference  
41 tetramethylsilane (TMS). When the amide nitrogen bears two substituents, the  $^1\text{H}$  and  $^{13}\text{C}$  NMR  
42 spectra show the presence of two different rotamers in equilibrium. Copies of  $^1\text{H}$  and  $^{13}\text{C}$  NMR  
43  
44  
45  
46  
47  
48  
49  
50  
51  
52  
53  
54  
55  
56  
57  
58  
59  
60

1  
2  
3 spectra are included in the Supporting Information. Low-resolution mass spectra were recorded on a  
4  
5 Finnigan LCQ DECA ThermoQuest mass spectrometer in electrospray positive and negative  
6  
7 ionization modes (ESI-MS). High-resolution mass spectra were recorded on a ThermoFisher  
8  
9 scientific Orbitrap XL<sup>TM</sup> mass spectrometer in electrospray positive ionization modes (ESI-MS).  
10  
11 Ultraviolet absorption spectra were recorded on a PerkinElmer EnSight<sup>TM</sup> Multimode Plate  
12  
13 Reader. Fluorescence spectra were recorded with a Gemini XS Molecular Device Spectramax  
14  
15 fluorescence Spectrophotometer. High performance liquid chromatography (HPLC) was performed  
16  
17 on a Shimadzu SPD 20A UV/VIS detector ( $\lambda = 220$  nm) using C-18 column Phenomenex Synergi  
18  
19 Fusion – RP 80A (75 x 4.60 mm; 4  $\mu$ m) at 25 °C using a mobile phase A (water + 0.1%  
20  
21 trifluoroacetic acid (TFA)) and B (MeCN + 0.1% TFA) at a flow rate of 1 mL min<sup>-1</sup>. The following  
22  
23 gradient was applied: isocratic elution for 1 min at 10% of solvent B, linear increase from 10% to  
24  
25 95% of solvent B over 10 min, hold at 95% solvent B for 3 min. The purity of all final compounds  
26  
27 was determined by HPLC, and it was found to be higher than 95%. Aldehydes **28** and **29** were  
28  
29 commercially available. The quinazoline-2-carboxylic acids **17** and **18**, the *N*-(4-  
30  
31 nitrobenzyl)ethanamine **24** and 4-((*N*-ethyl-4-phenylquinazoline-2-carboxamido)methyl)-phenyl 4-  
32  
33 methylbenzenesulfonate **7** were prepared as previously reported.<sup>23</sup>

34  
35  
36  
37  
38 **4-((4-(2-Chlorophenyl)-*N*-ethylquinazoline-2-carboxamido)methyl)-phenyl 4-**  
39  
40 **Methylbenzenesulfonate (8).** A solution of carboxylic acid **18** (305 mg, 1.07 mmol), HOBt (328  
41  
42 mg, 2.14 mmol), HBTU (812 mg, 2.14 mmol), and DIEA (0.76 mL, 4.28 mmol) in dry THF–DMF  
43  
44 (7:2, 9 mL) was added to a solution of amine **19** (327 mg, 1.07 mmol) in dry THF (3 mL) under N<sub>2</sub>  
45  
46 atmosphere. The reaction was stirred at room temperature overnight and then concentrated in vacuo.  
47  
48 The residue was dissolved in EtOAc (100 mL) and washed with NaHCO<sub>3</sub>, saturated aqueous  
49  
50 solution (3 × 30 mL) and brine. The organic solution was dried (Na<sub>2</sub>SO<sub>4</sub>), filtered, and concentrated  
51  
52 in vacuo. Purification by column chromatography on silica gel (EtOAc/ hexane, 7:3) provided  
53  
54 compound **8** as a white solid (520 mg, 85%); mp 68–71 °C. <sup>1</sup>H NMR (400 MHz, CDCl<sub>3</sub>):  $\delta$  = 8.17–  
55  
56 8.09 (m, 1H), 7.96–7.90 (m, 1H), 7.68–7.53 (m, 4H), 7.53–7.39 (m, 3H), 7.35–7.23 (m, 5H), 6.93,  
57  
58  
59  
60

6.87 (2d,  $J = 8.5$  Hz, 2H), 4.82–4.63, 4.45 (m, s, 2H), 3.56–3.44, 3.23 (m, q,  $J = 7.1$  Hz, 2H), 2.41 (s, 3H), 1.15, 1.07 ppm (2t,  $J = 7.1$  Hz, 3H).  $^{13}\text{C}$  NMR (100 MHz,  $\text{CDCl}_3$ ):  $\delta = 168.04, 167.99, 167.69, 167.09, 158.20, 158.10, 150.61, 150.51, 149.25, 149.09, 145.54, 145.50, 136.31, 135.79, 135.73, 135.59, 134.86, 134.82, 132.89, 132.84, 132.48, 131.09, 131.06, 131.00, 130.11, 130.07, 129.92, 129.88, 129.60, 129.42, 129.27, 129.20, 128.85, 128.81, 128.68, 128.63, 128.14, 127.14, 127.12, 127.07, 123.32, 123.22, 122.69, 122.61, 51.50, 47.17, 43.17, 40.19, 27.06, 21.86, 13.88, 12.50$  ppm. HRMS (ESI):  $m/z$  calculated for  $\text{C}_{31}\text{H}_{27}\text{ClN}_3\text{O}_4\text{S} + \text{H}^+$  [ $\text{M} + \text{H}^+$ ]: 572.1405. Found 572.1384.

**4-((*N*-Ethyl-4-phenylquinazoline-2-carboxamido)methyl)phenyl 4-methylbenzoate (9).**

Compound **9** was obtained as a white solid (291 mg, 58%) from acid **17** (250 mg, 1.00 mmol) and amine **20** (269 mg, 1.00 mmol), according to the procedure described for amide **8**; mp 70–72 °C.  $^1\text{H}$  NMR (400 MHz,  $\text{CDCl}_3$ ):  $\delta = 8.20$ – $8.13$  (m, 2H),  $8.11$ – $8.07$  (m, 2H),  $7.96$ – $7.93$  (m, 1H),  $7.84$ – $7.81$  (m, 1H),  $7.73$ – $7.71$  (m, 1H),  $7.66$ – $7.64$  (m, 1H),  $7.59$ – $7.53$  (m, 5H),  $7.31$  (d,  $J = 8.0$  Hz, 2H),  $7.22, 7.17$  (2d,  $J = 8.4$  Hz, 2H),  $4.89, 4.55$  (2s, 2H),  $3.61, 3.30$  (2q,  $J = 7.1$  Hz, 2H),  $2.46$  (s, 3H),  $1.27, 1.19$  ppm (2t,  $J = 7.1$  Hz, 3H).  $^{13}\text{C}$  NMR (100 MHz,  $\text{CDCl}_3$ ):  $\delta = 169.30, 167.92, 167.51, 165.38, 165.31, 158.40, 158.29, 151.21, 151.17, 150.73, 150.52, 144.65, 144.55, 136.87, 136.74, 134.79, 134.35, 134.29, 130.41, 130.38, 130.35, 129.71, 129.45, 129.43, 129.37, 129.27, 128.76, 128.73, 128.53, 128.46, 127.30, 126.95, 126.84, 122.61, 122.55, 122.07, 121.98, 51.55, 46.91, 42.84, 39.91, 21.91, 13.83, 12.48$  ppm. HRMS (ESI):  $m/z$  calculated for  $\text{C}_{32}\text{H}_{28}\text{N}_3\text{O}_3 + \text{H}^+$  [ $\text{M} + \text{H}^+$ ]: 502.2125. Found 502.2109.

**4-((4-(2-Chlorophenyl)-*N*-ethylquinazoline-2-carboxamido)methyl)phenyl 4-methylbenzoate (10).** Compound **10** was obtained as a white solid (322 mg, 60%) from acid **18** (285 mg, 1.00 mmol) and amine **20** (270 mg, 1.00 mmol), according to the procedure described for amide **8**; mp 80–82 °C.  $^1\text{H}$  NMR (400 MHz,  $\text{CDCl}_3$ ):  $\delta = 8.21$ – $8.16$  (m, 1H),  $8.10$ – $8.06$  (m, 2H),  $7.99$ – $7.92$  (m, 1H),  $7.70$ – $7.58$  (m, 2H),  $7.56$ – $7.39$  (m, 6H),  $7.31$  (d,  $J = 7.9$  Hz, 2H),  $7.21, 7.14$  (2d,  $J = 8.4$  Hz, 2H),  $4.96$ – $4.79, 4.59$ – $4.51$  (2m, 2H),  $3.67$ – $3.54, 3.30$  (m, q,  $J = 7.1$  Hz, 2H),  $2.45$  (s, 3H),  $1.26, 1.15$

1  
2  
3 ppm (2t,  $J = 7.1$  Hz, 3H).  $^{13}\text{C}$  NMR (100 MHz,  $\text{CDCl}_3$ ):  $\delta = 168.04, 167.66, 167.20, 165.37,$   
4  
5 165.28, 158.40, 158.31, 150.72, 150.65, 150.56, 150.53, 144.64, 144.55, 135.81, 135.71, 134.80,  
6  
7 134.73, 134.18, 132.94, 131.17, 131.06, 131.03, 131.01, 130.37, 130.34, 130.08, 129.72 129.45,  
8  
9 129.43, 129.33, 129.27, 128.76, 128.70, 127.12, 127.09, 127.05, 126.96, 126.84, 123.31, 123.22,  
10  
11 122.07, 121.98, 51.54, 47.06, 42.85, 40.01, 21.91, 13.82, 12.50 ppm. HRMS (ESI):  $m/z$  calculated  
12  
13 for  $\text{C}_{32}\text{H}_{27}\text{ClN}_3\text{O}_3 + \text{H}^+$  [ $\text{M} + \text{H}^+$ ]: 536.1735. Found 536.1723.

14  
15  
16 ***N*-Ethyl-*N*-(4-(4-methylbenzamido)benzyl)-4-phenylquinazoline-2-carboxamide (11).**

17  
18 Compound **11** was obtained as a yellow solid (340 mg, 68%) from acid **17** (250 mg, 1.00 mmol)  
19  
20 and amine **21** (382 mg, 1.00 mmol), according to the procedure described for amide **8**; mp 100–102  
21  
22 °C.  $^1\text{H}$  NMR (400 MHz,  $\text{CDCl}_3$ ):  $\delta = 8.32, 8.05$  (2br s, 1H, exchangeable with deuterium oxide),  
23  
24 8.15–8.11 (m, 2H), 7.95–7.90 (m, 1H), 7.78–7.70 (m, 5H), 7.66–7.61 (m, 2H), 7.58–7.51 (m, 3H),  
25  
26 7.47–7.4 (m, 2H), 7.22, 7.15 (2d,  $J = 7.9$  Hz, 2H), 4.85, 4.50 (2s, 2H), 3.58, 3.27 (2q,  $J = 7.1$  Hz,  
27  
28 2H), 2.38, 2.33 (2s, 3H), 1.24, 1.19 ppm (t,  $J = 7.1$  Hz, 3H).  $^{13}\text{C}$  NMR (100 MHz,  $\text{CDCl}_3$ ):  $\delta =$   
29  
30 169.27, 169.20, 168.03, 167.52, 165.84, 165.75, 158.32, 151.13, 142.45, 142.14, 137.95, 137.83,  
31  
32 136.75, 136.73, 134.33, 134.27, 132.98, 132.54, 132.16, 132.10, 130.43, 130.37, 129.49, 129.32,  
33  
34 129.27, 128.93, 128.74, 128.70, 128.50, 128.43, 127.28, 127.22, 127.19, 122.49, 120.78, 120.34,  
35  
36 51.72, 47.09, 42.8, 39.88, 21.61, 21.58, 13.82, 12.50 ppm. HRMS (ESI):  $m/z$  calculated for  
37  
38  $\text{C}_{32}\text{H}_{29}\text{N}_4\text{O}_2 + \text{H}^+$  [ $\text{M} + \text{H}^+$ ]: 501.2285. Found 501.2275.

39  
40  
41  
42  
43 ***4*-(2-Chlorophenyl)-*N*-ethyl-*N*-(4-(4-methylbenzamido)benzyl)quinazoline-2-carboxamide**

44  
45 **(12).** Compound **12** was obtained as a yellow solid (396 mg, 74%) from acid **18** (285 mg, 1.00  
46  
47 mmol) and amine **21** (382 mg, 1.00 mmol), according to the procedure described for amide **8**; mp  
48  
49 110–112 °C.  $^1\text{H}$  NMR (400 MHz,  $\text{CDCl}_3$ ):  $\delta = 8.18$ –8.15 (m, 1H), 8.14, 7.99 (br s, 1H,  
50  
51 exchangeable with deuterium oxide), 7.96–7.93 (m, 1H), 7.78–7.75 (m, 2H), 7.68–7.56 (m, 4H),  
52  
53 7.56–7.48 (m, 2H), 7.46–7.38 (m, 4H), 7.26–7.21 (m, 2H), 4.90–4.76, 4.51 (m, s, 2H), 3.62–3.52,  
54  
55 3.27 (m, q,  $J = 7.1$  Hz, 2H), 2.39, 2.38 (2s, 3H), 1.22, 1.14 ppm (2t,  $J = 7.1$  Hz, 3H).  $^{13}\text{C}$  NMR (100  
56  
57 MHz,  $\text{CDCl}_3$ ):  $\delta = 168.02, 167.94, 167.70, 165.80, 165.73, 158.37, 158.33, 150.60, 150.53, 142.49,$   
58  
59  
60

1  
2  
3 142.31, 137.91, 137.69, 135.76, 135.69, 134.78, 134.72, 133.07, 132.91, 132.48, 132.19, 132.10,  
4  
5 131.14, 131.03, 131.01, 130.07, 130.05, 129.52, 129.45, 129.31, 129.28, 129.24, 128.96, 128.74,  
6  
7 128.69, 127.24, 127.19, 127.12, 127.09, 127.07, 127.03, 123.25, 123.18, 120.69, 120.32, 51.69,  
8  
9 47.22, 42.83, 39.95, 21.61, 13.82, 12.51 ppm. HRMS (ESI):  $m/z$  calculated for  $C_{32}H_{28}ClN_4O_2 + H^+$   
10  
11  $[M + H^+]$ : 535.1895. Found 535.1889.

12  
13  
14 **(((4-Phenylquinazoline-2-carbonyl)azanediyl)bis(methylene))bis(4,1-phenylene) bis(4-**  
15 **methylbenzenesulfonate) (13).** Compound **13** was obtained as a yellow solid (539 mg, 70%) from  
16  
17 acid **17** (250 mg, 1.00 mmol) and amine **22** (538 mg, 1.00 mmol), according to the procedure  
18  
19 described for amide **8**; mp 115–117 °C.  $^1H$  NMR (400 MHz,  $CDCl_3$ ):  $\delta$  = 8.17–8.12 (m, 2H), 7.97–  
20  
21 7.93 (m, 1H), 7.73–7.66 (m, 7H), 7.58–7.55 (m, 3H), 7.33–7.26 (m, 8H), 6.96, 6.92 (2d,  $J$  = 8.5 Hz,  
22  
23 4H), 4.64, 4.37 (2s, 4H), 2.46 ppm (s, 6H).  $^{13}C$  NMR (100 MHz,  $CDCl_3$ ):  $\delta$  = 169.37, 167.99,  
24  
25 157.65, 151.15, 149.35, 149.22, 145.62, 145.59, 136.58, 135.42, 134.99, 134.51, 132.66, 132.56,  
26  
27 130.59, 130.35, 130.05, 129.98, 129.95, 129.59, 129.34, 128.78, 128.67, 128.60, 127.36, 122.77,  
28  
29 122.70, 122.62, 50.91, 46.67, 21.89 ppm. HRMS (ESI):  $m/z$  calculated for  $C_{43}H_{36}N_3O_7S_2 + H^+$   $[M +$   
30  
31  $H^+]$ : 770.1989. Found 770.1976.

32  
33  
34 **(((4-Phenylquinazoline-2-carbonyl)azanediyl)bis(methylene))bis(4,1-phenylene) bis(4-**  
35 **methylbenzoate) (14).** Compound **14** was obtained as a yellow solid (467 mg, 67%) from acid **17**  
36  
37 (250 mg, 1.00 mmol) and amine **23** (465 mg, 1.00 mmol), according to the procedure described for  
38  
39 amide **8**; mp 120–122 °C.  $^1H$  NMR (400 MHz,  $CDCl_3$ ):  $\delta$  = 8.19–8.15 (m, 2H), 8.11–8.08 (m, 4H),  
40  
41 7.97–7.93 (m, 1H), 7.76–7.73 (m, 2H), 7.67–7.63 (m, 1H), 7.58–7.55 (m, 3H), 7.53–7.48 (m, 4H),  
42  
43 7.32 (d,  $J$  = 8.0 Hz, 4H), 7.23, 7.18 (2d,  $J$  = 8.4 Hz, 4H), 4.79, 4.47 (2s, 4H), 2.46 ppm (s, 6H).  $^{13}C$   
44  
45 NMR (100 MHz,  $CDCl_3$ ):  $\delta$  = 169.17, 167.92, 165.24, 165.16, 157.88, 151.09, 150.67, 150.51,  
46  
47 144.51, 144.42, 136.57, 134.22, 133.98, 133.49, 130.31, 130.25, 130.22, 130.02, 129.32, 129.29,  
48  
49 128.59, 128.48, 127.17, 126.81, 126.72, 122.47, 122.01, 121.96, 50.59, 46.30, 21.77 ppm. HRMS  
50  
51 (ESI):  $m/z$  calculated for  $C_{45}H_{36}N_3O_5 + H^+$   $[M + H^+]$ : 698.2649. Found 698.2640.  
52  
53  
54  
55  
56  
57  
58  
59  
60

***N*-(4-(4-Nitrobenzo[*c*][1,2,5]oxadiazol-7-ylamino)butyl)-4-(2-chlorophenyl)quinazoline-2-carboxamide (15).** To a solution of amine **40** (355 mg, 0.28 mmol) in dry DMF (10 mL), a solution of 4-chloro-7-nitrobenzofurazan (55 mg, 0.28 mmol) in dry DMF (1 mL) was added dropwise. After addition of a CH<sub>2</sub>Cl<sub>2</sub> solution (1 mL) of TEA (0.04 mL, 0.30 mmol), the reaction mixture was stirred at room temperature overnight and then concentrated in vacuo. The residue was taken up with 0 °C cooled water (30 mL) and extracted with CH<sub>2</sub>Cl<sub>2</sub> (3 × 30 mL). The combined organic phases were washed with brine (10 mL), dried (Na<sub>2</sub>SO<sub>4</sub>), filtered, and concentrated in vacuo. Purification by column chromatography on silica gel (EtOAc) provided compound **15** as a yellow-brownish solid (104 mg, 72%); mp 57–59 °C. <sup>1</sup>H NMR (400 MHz, DMSO-*d*<sub>6</sub>): δ = 9.58 (t, *J* = 5.1 Hz, 1H, exchangeable with deuterium oxide), 9.05 (t, *J* = 6.0 Hz, 1H, exchangeable with deuterium oxide), 8.46 (d, *J* = 8.0 Hz, 1H), 8.23 (d, *J* = 8.4 Hz, 1H), 8.17–8.12 (m, 1H), 7.84–7.80 (m, 1H), 7.74–7.72 (m, 1H), 7.69–7.59 (m, 4H), 6.45 (d, *J* = 9.2 Hz, 1H), 3.54–3.53 (m, 2H), 3.42 (q, *J* = 9.6 Hz, 2H), 1.76–1.71 ppm (m, 4H). <sup>13</sup>C NMR (100 MHz, DMSO-*d*<sub>6</sub>): δ = 167.73, 163.14, 154.54, 150.17, 135.85, 135.70, 132.01, 131.93, 131.69, 130.34, 130.10, 129.41, 127.97, 127.06, 123.42, 26.99, 21.22 ppm. HRMS (ESI): *m/z* calculated for C<sub>25</sub>H<sub>20</sub>ClN<sub>7</sub>O<sub>4</sub> + H<sup>+</sup> [M + H<sup>+</sup>]: 517.1265. Found 517.1272.

***N*-(6-(4-Nitrobenzo[*c*][1,2,5]oxadiazol-7-ylamino)hexyl)-4-(2-chlorophenyl)quinazoline-2-carboxamide (16).** Compound **16** was obtained as a yellow-brownish solid (114 mg, 75%) from amine **41** (107 mg, 0.28 mmol), according to the procedure described for compound **15**; mp 57–58 °C. <sup>1</sup>H NMR (400 MHz, DMSO-*d*<sub>6</sub>): δ = 9.57 (br s, 1H, exchangeable with deuterium oxide), 9.00 (t, *J* = 6.0 Hz, 1H, exchangeable with deuterium oxide), 8.49 (d, *J* = 8.8 Hz, 1H), 8.24 (d, *J* = 8.4 Hz, 1H), 8.16–8.12 (m, 1H), 7.84–7.80 (m, 1H), 7.74–7.72 (m, 1H), 7.69–7.59 (m, 4H), 6.41 (d, *J* = 8.8 Hz, 1H), 3.47–3.45 (m, 2H), 3.39–3.34 (m, 2H), 1.72–1.69 (m, 2H), 1.62–1.58 (m, 2H), 1.41–1.39 ppm (m, 4H). <sup>13</sup>C NMR (100 MHz, DMSO-*d*<sub>6</sub>): δ = 167.72, 163.04, 154.64, 150.19, 135.82, 135.72, 132.01, 131.93, 131.71, 130.31, 130.10, 129.44, 127.98, 127.05, 123.42, 29.47, 26.60 ppm. HRMS (ESI): *m/z* calculated for C<sub>27</sub>H<sub>24</sub>ClN<sub>7</sub>O<sub>4</sub> + H<sup>+</sup> [M + H<sup>+</sup>]: 545.1578. Found 545.1572.

1  
2  
3 **4-((Ethylamino)methyl)phenyl 4-methylbenzenesulfonate (19)**. To a solution of 4-  
4 formylphenyl 4-methylbenzenesulfonate **28** (914 mg, 3.31 mmol) in dry ethanol (10 mL) was added  
5 ethylamine (2 M solution in THF, 1.80 mL, 3.64 mmol) under a nitrogen atmosphere. After stirring  
6 at room temperature for 12 h, the mixture was cooled at 0 °C, and NaBH<sub>4</sub> was added portion wise  
7 until disappearance of the intermediate imine (TLC analysis). The reaction mixture, after addition  
8 of water (20 mL), was concentrated in vacuo and extracted with EtOAc (3 × 40 mL). The combined  
9 organic phases were washed with a saturated solution of NaHCO<sub>3</sub> (3 × 20 mL) and brine (10 mL),  
10 dried (Na<sub>2</sub>SO<sub>4</sub>), filtered, and concentrated in vacuo to yield the title compound as a pale-yellow oil  
11 (970 mg, 96%). <sup>1</sup>H NMR (400 MHz, CDCl<sub>3</sub>): δ = 7.69 (d, *J* = 8.1 Hz, 2H), 7.30 (d, *J* = 8.1 Hz, 2H),  
12 7.23 (d, *J* = 8.4 Hz, 2H), 6.92 (d, *J* = 8.4 Hz, 2H), 3.74 (s, 2H), 2.65 (q, *J* = 7.1 Hz, 2H), 2.53 (s,  
13 3H), 1.62 (br s, 1H, exchangeable with deuterium oxide), 1.12 ppm (t, *J* = 7.1 Hz, 3H). MS (ESI)  
14 *m/z* (%): 306 (100) [M + H]<sup>+</sup>.  
15  
16  
17  
18  
19  
20  
21  
22  
23  
24  
25  
26  
27  
28

29 **4-((Ethylamino)methyl)phenyl 4-methylbenzoate (20)**. Compound **20** was obtained as a pale-  
30 yellow oil (637 mg, 71%) from aldehyde **29** (800 mg, 3.33 mmol) and ethylamine (1.83 mL, 3.66  
31 mmol), according to the procedure described for amine **19**. <sup>1</sup>H NMR (400 MHz, CDCl<sub>3</sub>): δ = 8.09  
32 (d, *J* = 8.0 Hz, 2H), 7.38 (d, *J* = 8.4 Hz, 2H), 7.31 (d, *J* = 8.0 Hz, 2H), 7.16 (d, *J* = 8.4 Hz, 2H),  
33 5.42–5.17 (m, 1H, exchangeable with deuterium oxide), 3.82 (s, 2H), 2.71 (q, *J* = 7.1 Hz, 2H), 2.45  
34 (s, 3H), 1.15 ppm (t, *J* = 7.1 Hz, 3H). MS (ESI) *m/z* (%): 270 (100) [M + H]<sup>+</sup>.  
35  
36  
37  
38  
39  
40  
41  
42

43 **m-(4-((Ethylamino)methyl)phenyl)-4-methylbenzamide trifluoroacetate (21)**. Compound **27**  
44 (800 mg, 2.17 mmol) was treated with a mixture of TFA and CH<sub>2</sub>Cl<sub>2</sub> (3:7, 14 mL). After stirring at  
45 room temperature for 30 min the mixture was concentrated in vacuo to give the title compound as a  
46 hygroscopic solid (822 mg, 99%). <sup>1</sup>H NMR (400 MHz, DMSO-*d*<sub>6</sub>): δ = 10.28 (br s, 1H,  
47 exchangeable with deuterium oxide), 8.70 (br s, 2H, exchangeable with deuterium oxide), 7.88 (d, *J*  
48 = 8.2 Hz, 2H), 7.83 (d, *J* = 7.9 Hz, 2H), 7.45 (d, *J* = 8.2 Hz, 2H), 7.35 (d, *J* = 7.9 Hz, 2H), 4.10 (s,  
49 2H), 2.97 (q, *J* = 7.1 Hz, 2H), 2.39 (s, 3H), 1.21 ppm (t, *J* = 7.1 Hz, 3H). MS (ESI) *m/z* (%): 269  
50 (100) [M + H]<sup>+</sup>.  
51  
52  
53  
54  
55  
56  
57  
58  
59  
60

1  
2  
3 (Azanediylbis(methylene))bis(4,1-phenylene) bis(4-methylbenzenesulfonate) (**22**). Compound  
4  
5 **22** was obtained as a pale-yellow oil (944 mg, 97%) from aldehyde **28** (500 mg, 1.81 mmol) and  
6  
7 amine **36** (552 mg, 1.99 mmol) according to the procedure described for compound **19**. <sup>1</sup>H NMR  
8  
9 (400 MHz, CDCl<sub>3</sub>): δ = 7.71 (d, *J* = 8.0 Hz, 4H), 7.30 (d, *J* = 8.2 Hz, 4H), 7.24 (d, *J* = 8.2 Hz, 4H),  
10  
11 6.93 (d, *J* = 8.0 Hz, 4H), 3.73 (s, 4H), 2.45 ppm (s, 6H). MS (ESI) *m/z* (%): 538 (100) [M + H]<sup>+</sup>.  
12  
13

14 (Azanediylbis(methylene))bis(4,1-phenylene) bis(4-methylbenzoate) (**23**). Compound **23** was  
15  
16 obtained as a colourless oil (881 mg, 91%) from aldehyde **29** (500 mg, 2.08 mmol) and amine **36**  
17  
18 (550 mg, 2.29 mmol) according to the procedure described for compound **19**. <sup>1</sup>H NMR (400 MHz,  
19  
20 CDCl<sub>3</sub>): δ = 8.09 (d, *J* = 8.0 Hz, 4H), 7.41 (d, *J* = 7.9 Hz, 4H), 7.31 (d, *J* = 8.0 Hz, 4H), 7.18 (d, *J* =  
21  
22 7.9 Hz, 4H), 3.85 (s, 4H), 2.45 ppm (s, 6H). MS (ESI) *m/z* (%): 466 (100) [M + H]<sup>+</sup>.  
23  
24

25 *tert*-Butyl ethyl(4-nitrobenzyl)carbamate (**25**). *N*-(4-Nitrobenzyl)ethanamine **24**<sup>23</sup> (1.09 g, 6.05  
26  
27 mmol) was dissolved in ethyl acetate (20 mL) and di-*tert*-butyl dicarbonate (1.32 g, 6.05 mmol) was  
28  
29 added. After stirring at room temperature for 1 h, to the mixture water (50 mL) was added. The  
30  
31 organic layer was separated, and the aqueous phase was extracted with ethyl acetate (3 × 70 mL).  
32  
33 The combined organic phases were washed with brine (10 mL), dried (Na<sub>2</sub>SO<sub>4</sub>), filtered, and  
34  
35 concentrated in vacuo. The residue was purified by silica gel chromatography (EtOAc/hexanes, 1:9)  
36  
37 to give the title compound as an orange oil (1.56 g, 92%). <sup>1</sup>H NMR (400 MHz, CDCl<sub>3</sub>): δ = 8.21 (d,  
38  
39 *J* = 8.4 Hz, 2H), 7.41 (d, *J* = 8.4 Hz, 2H), 4.52 (s, 2H), 3.53–3.11 (m, 2H), 1.47 (br s, 9H), 1.12 ppm  
40  
41 (t, *J* = 7.1 Hz, 3H). MS (ESI) *m/z* (%): 281 (100) [M + H]<sup>+</sup>.  
42  
43  
44

45 *tert*-Butyl (4-aminobenzyl)(ethyl)carbamate (**26**). To an ice cooled solution of *tert*-butyl  
46  
47 ethyl(4-nitrobenzyl)carbamate **25** (1.00 g, 3.57 mmol) in AcOH (70 mL) zinc powder (2.33 g, 35.7  
48  
49 mmol) was added. After stirring at room temperature for 10 min, the solid was filtered off, and the  
50  
51 solvent was evaporated. The residue was taken up with EtOAc (200 mL) and washed with NaHCO<sub>3</sub>  
52  
53 saturated aqueous solution twice. The organic phase was dried (Na<sub>2</sub>SO<sub>4</sub>), filtered, and concentrated  
54  
55 in vacuo to give the title compound as a yellow oil (805 mg, 90%). <sup>1</sup>H NMR (400 MHz, CDCl<sub>3</sub>): δ  
56  
57 = 6.92 (d, *J* = 8.0 Hz, 2H), 6.50 (d, *J* = 8.0 Hz, 2H), 4.98 (s, 2H), 4.16 (s, 2H), 3.10 (br s, 2H,  
58  
59  
60

exchangeable with deuterium oxide), 1.42 (s, 9H), 0.94 ppm (t,  $J = 7.7$  Hz, 3H). MS (ESI)  $m/z$  (%): 273 (100)  $[M + Na]^+$ .

***tert*-Butyl ethyl(4-(4-methylbenzamido)benzyl)carbamate (27).** Compound **27** was obtained as a yellow oil (846 mg, 72%) from 4-methylbenzoic acid (434 mg, 3.19 mmol) and amine **26** (800 mg, 3.19 mmol), according to the procedure described for amide **8**.  $^1\text{H}$  NMR (400 MHz,  $\text{CDCl}_3$ ):  $\delta = 7.98$  (br s, 1H, exchangeable with deuterium oxide), 7.78 (d,  $J = 7.7$  Hz, 2H), 7.60 (d,  $J = 7.9$  Hz, 2H), 7.32–7.19 (m, 4H), 4.41 (s, 2H), 3.37–3.11 (m, 2H), 2.43 (s, 3H), 1.49 (s, 9H), 1.07 ppm (t,  $J = 6.8$  Hz, 3H). MS (ESI)  $m/z$  (%): 369 (100)  $[M + H]^+$ .

**4-(Hydroxymethyl)phenyl 4-methylbenzenesulfonate (30).**<sup>37</sup> A solution of 4-formylphenyl 4-methylbenzenesulfonate **28** (914 mg, 3.31 mmol) in methanol (10 mL) was refrigerated to 0 °C, and  $\text{NaBH}_4$  was added portion wise until disappearance of the starting material (TLC analysis). The reaction mixture, after addition of water (20 mL), was concentrated in vacuo and extracted with EtOAc (3  $\times$  40 mL). The combined organic phases were washed with a saturated solution of  $\text{NaHCO}_3$  (3  $\times$  20 mL) and brine (10 mL), dried ( $\text{Na}_2\text{SO}_4$ ), filtered, and concentrated in vacuo to yield the title compound as a colourless oil (857 mg, 93%).  $^1\text{H}$  NMR (400 MHz,  $\text{CDCl}_3$ ):  $\delta = 7.71$  (d,  $J = 8.5$  Hz, 2H), 7.36–7.24 (m, 4H), 6.97 (d,  $J = 8.5$  Hz, 2H), 4.66 (s, 2H), 2.45 ppm (s, 3H). MS (ESI)  $m/z$  (%): 279 (100)  $[M + H]^+$ .

**4-(Hydroxymethyl)phenyl 4-methylbenzoate (31).**<sup>38</sup> Compound **31** was obtained as a colourless oil (754 mg, 94%) from aldehyde **29** (795 mg, 3.31 mmol), according to the procedure described for alcohol **30**.  $^1\text{H}$  NMR (400 MHz,  $\text{CDCl}_3$ ):  $\delta = 8.09$  (d,  $J = 7.9$  Hz, 2H), 7.44 (d,  $J = 8.0$  Hz, 2H), 7.31 (d,  $J = 7.9$  Hz, 2H), 7.21 (d,  $J = 8.0$  Hz, 2H), 4.73 (d,  $J = 5.8$  Hz, 2H), 2.46 ppm (s, 3H). MS (ESI)  $m/z$  (%): 243 (100)  $[M + H]^+$ .

**4-(((Methylsulfonyl)oxy)methyl)phenyl 4-methylbenzenesulfonate (32).** To a solution of 4-(hydroxymethyl)phenyl 4-methylbenzenesulfonate **31** (800 mg, 2.87 mmol) and trimethylamine (0.48 mL, 3.44 mmol) in dry  $\text{CH}_2\text{Cl}_2$  (23 mL), methanesulfonyl chloride (0.27 mL, 3.44 mmol) was added at 0 °C. After stirring at room temperature for 45 min, the solvent was evaporated and the

1  
2  
3 residue was taken up with water (20 mL) and extracted with CH<sub>2</sub>Cl<sub>2</sub> (3 x 20 mL). The combined  
4  
5 organic phases were washed with 1N HCl (2 x 10 mL), NaHCO<sub>3</sub>, saturated aqueous solution (2 x 10  
6  
7 mL), and brine (10 mL), dried (Na<sub>2</sub>SO<sub>4</sub>), filtered, and concentrated in vacuo to give mesylate **38**,  
8  
9 which was used without further purification in the subsequent reaction.  
10

11 **4-(((Methylsulfonyl)oxy)methyl)phenyl 4-methylbenzoate (33)**. Compound **33** was obtained  
12  
13 from alcohol **31**, according to the procedure described for mesylate **32** and used without further  
14  
15 purification in the subsequent reaction.  
16

17 **4-(Azidomethyl)phenyl 4-methylbenzenesulfonate (34)**. To a solution of **32** (1.02 g, 2.87  
18  
19 mmol) in DMF (10 mL) sodium azide (560 mg, 8.61 mmol) was added. After stirring at 80 °C for  
20  
21 1h, water (20 mL) was added and the mixture was extracted with CHCl<sub>3</sub> (3 × 20 mL). The  
22  
23 combined organic phases were washed with NaHCO<sub>3</sub> saturated aqueous solution (20 mL) and brine  
24  
25 (20 mL), dried (Na<sub>2</sub>SO<sub>4</sub>), filtered, and concentrated in vacuo. The residue was purified by silica gel  
26  
27 chromatography (EtOAc/ hexanes, 7:3) to give the title compounds as a pale-yellow solid (766 mg,  
28  
29 88%); mp 100–102 °C. <sup>1</sup>H NMR (400 MHz, CDCl<sub>3</sub>): δ = 7.70 (d, *J* = 8.4 Hz, 2H), 7.31 (d, *J* = 8.1  
30  
31 Hz, 2H), 7.24 (d, *J* = 8.1 Hz, 2H), 7.00 (d, *J* = 8.4 Hz, 2H), 4.32 (s, 2H), 2.45 ppm (s, 3H). MS  
32  
33 (ESI) *m/z* (%): 304 (100) [M + H]<sup>+</sup>.  
34  
35  
36  
37

38 **4-(Azidomethyl)phenyl 4-methylbenzoate (35)**. Compound **35** was obtained as a pale-yellow  
39  
40 solid (698 mg, 91%) from mesylate **33** (919 mg, 2.87 mmol), according to the procedure described  
41  
42 for azide **34**. Mp 107–109 °C. <sup>1</sup>H NMR (400 MHz, CDCl<sub>3</sub>): δ = 8.09 (d, *J* = 7.9 Hz, 2H), 7.39 (d, *J*  
43  
44 = 8.4 Hz, 2H), 7.32 (d, *J* = 7.9 Hz, 2H), 7.24 (d, *J* = 8.4 Hz, 2H), 4.38 (s, 2H), 2.46 ppm (s, 3H).  
45  
46 MS (ESI) *m/z* (%): 268 (100) [M + H]<sup>+</sup>.  
47  
48

49 **4-(Aminomethyl)phenyl 4-methylbenzenesulfonate (36)**. A suitable glass vial was charged  
50  
51 with 50 mL of an azide **34** solution (0.05 M in MeOH). The reaction parameters (full-H<sub>2</sub> mode, 30  
52  
53 °C, 10 bar and 1 mL min<sup>-1</sup> flow rate) were selected on the H-Cube-Pro™ hydrogenator fitted with a  
54  
55 30 mm 10% Pd/C CatCart. Firstly, MeOH was pumped through the system until the instrument had  
56  
57 achieved the desired reaction parameters and then the sample inlet line was switched to the vial  
58  
59  
60

1  
2  
3 containing the substrate. A total reaction volume of 55 mL was collected and the cartridge was  
4  
5 washed with MeOH for 5 min. Evaporation of the solvent afforded the desired amine as a colourless  
6  
7 oil (624 mg, 90%).  $^1\text{H}$  NMR (400 MHz,  $\text{CDCl}_3$ ):  $\delta$  = 7.71 (d,  $J$  = 7.9 Hz, 2H), 7.31 (d,  $J$  = 8.2 Hz,  
8  
9 2H), 7.23 (d,  $J$  = 8.2 Hz, 2H), 6.94 (d,  $J$  = 7.9 Hz, 2H), 3.84 (s, 2H), 2.45 ppm (s, 3H). MS (ESI)  
10  
11  $m/z$  (%): 278 (100)  $[\text{M} + \text{H}]^+$ .

12  
13  
14 **4-(Aminomethyl)phenyl 4-methylbenzoate (37)**. Compound **37** was obtained as a colourless oil  
15  
16 (563 mg, 96%) from azide **35** (650 mg, 2.43 mmol), according to the procedure described for amine  
17  
18 **36**.  $^1\text{H}$  NMR (400 MHz,  $\text{CDCl}_3$ ):  $\delta$  = 8.09 (d,  $J$  = 8.1 Hz, 2H), 7.38 (d,  $J$  = 8.0 Hz, 2H), 7.31 (d,  $J$  =  
19  
20 8.1 Hz, 2H), 7.17 (d,  $J$  = 8.0 Hz, 2H), 3.90 (s, 2H), 2.45 ppm (s, 3H). MS (ESI)  $m/z$  (%): 242 (100)  
21  
22  $[\text{M} + \text{H}]^+$ .

23  
24  
25 **tert-Butyl 4-(4-(2-chlorophenyl)quinazoline-2-carboxamido)butylcarbamate (38)**. A solution  
26  
27 of 4-phenylquinazoline-2-carboxylic acid **18** (568 mg, 2.00 mmol) in excess thionyl chloride (25  
28  
29 mL) was refluxed for 2 h under a nitrogen atmosphere. After the solution was cooled at room  
30  
31 temperature, the excess thionyl chloride was removed at reduced pressure and the crude material  
32  
33 dried under vacuum. To the residue, dissolved in dry THF (30 mL) and cooled to 0 °C, was added  
34  
35 dropwise a mixture of *N*-Boc-1,4-butanediamine (377 mg, 2.00 mmol) and triethylamine (0.28 mL,  
36  
37 2.00 mmol) in dry THF (10 mL). The mixture was stirred at room temperature for 48 h, filtered, and  
38  
39 evaporated. The crude residue was dissolved in DCM (20 mL), washed with 1N HCl, saturated  
40  
41  $\text{NaHCO}_3$ , and water, dried, and concentrated in vacuum. Purification by column chromatography on  
42  
43 silica gel (hexane–EtOAc: 3-7) provided the title compound as a white solid; mp 68–70 °C.  $^1\text{H}$   
44  
45 NMR (400 MHz,  $\text{CDCl}_3$ ):  $\delta$  = 8.35–8.32 (m, 2H, 1H exchangeable with deuterium oxide), 8.02–  
46  
47 7.98 (m, 1H), 7.75–7.66 (m, 2H), 7.60 (d,  $J$  = 8.0 Hz, 1H), 7.57–7.28 (m, 3H), 4.64 (s, 1H,  
48  
49 exchangeable with deuterium oxide), 3.60 (q,  $J$  = 9.8 Hz, 2H), 3.20–3.18 (m, 2H), 1.75–1.71 (m,  
50  
51 2H), 1.64–1.60 (m, 2H), 1.44 ppm (s, 9H). MS (ESI)  $m/z$  (%): 455 (100)  $[\text{M} + \text{H}]^+$ , 456 (36)  $[\text{M} + \text{H}$   
52  
53  $+ 1]^+$ .

**tert-Butyl 6-(4-(2-chlorophenyl)quinazoline-2-carboxamido)hexylcarbamate (39).** Compound **39** was obtained as a white solid (676 mg, 70%) from acid **18** (568 mg, 2.00 mmol) and *N*-Boc-1,6-hexanediamine (433 mg, 2.00 mmol), according to the procedure described for amide **38**; mp 51–54 °C. <sup>1</sup>H NMR (400 MHz, CDCl<sub>3</sub>): δ = 8.35–8.31 (m, 2H, 1H exchangeable with deuterium oxide), 7.99–7.96 (m, 1H), 7.72 (d, *J* = 7.6 Hz, 1H), 7.67–7.63 (m, 1H), 7.58 (d, *J* = 2.4 Hz, 1H), 7.53–7.47 (m, 3H), 4.60 (s, 1H, exchangeable with deuterium oxide), 3.55 (q, *J* = 9.8 Hz, 2H), 3.10–3.09 (m, 2H), 1.69–1.64 (m, 2H), 1.50–1.33 ppm (m, 15H). MS (ESI) *m/z* (%): 483 (100) [M + H]<sup>+</sup>, 484 (36) [M + H + 1]<sup>+</sup>.

***N*-(4-Aminobutyl)-4-(2-chlorophenyl)quinazoline-2-carboxamide (40).** A stirred solution of compound **38** (600 mg, 1.32 mmol) in dry CH<sub>2</sub>Cl<sub>2</sub> (10 mL) was treated dropwise with TFA (20 mL). After stirring at room temperature for 3 h, the reaction mixture was concentrated in vacuo. The solid residue was taken up with water, cooled in an ice bath, treated with a 3M solution of NaOH (20 mL) and extracted with CH<sub>2</sub>Cl<sub>2</sub> (3 × 40 mL). The combined organic phases were washed with brine (10 mL), dried (Na<sub>2</sub>SO<sub>4</sub>), filtered, and concentrated in vacuo to yield the title compound as a colorless oil (347 mg, 74%). <sup>1</sup>H NMR (400 MHz, CDCl<sub>3</sub>): δ = 8.47–8.44 (m, 1H, exchangeable with deuterium oxide), 8.35 (d, *J* = 8.4 Hz, 1H), 8.01–7.98 (m, 1H), 7.74–7.66 (m, 2H), 7.61–7.49 (m, 4H), 3.60 (q, *J* = 9.4 Hz, 2H), 2.90–2.81 (m, 4H, 2H exchangeable with deuterium oxide), 1.76–1.62 ppm (m, 4H). MS (ESI) *m/z* (%): 355 (100) [M + H]<sup>+</sup>, 356 (34) [M + H + 1]<sup>+</sup>.

***N*-(6-Aminoethyl)-4-(2-chlorophenyl)quinazoline-2-carboxamide (41).** Compound **41** was obtained as a colorless oil (408 mg, 86%) from derivative **39** (600 mg, 1.24 mmol), according to the procedure described for amine **40**. <sup>1</sup>H NMR (400 MHz, CDCl<sub>3</sub>): δ = 8.35–8.33 (m, 2H, 1H exchangeable with deuterium oxide), 8.03–7.98 (m, 1H), 7.75–7.68 (m, 2H), 7.62–7.50 (m, 4H), 3.58–3.55 (m, 2H), 3.38 (br s, 2H, exchangeable with deuterium oxide), 2.81–2.77 (m, 2H), 1.71–1.67 (m, 2H), 1.59–1.55 (m, 2H), 1.42–1.35 ppm (m, 4H). MS (ESI) *m/z* (%): 383 (100) [M + H]<sup>+</sup>, 384 (34) [M + H + 1]<sup>+</sup>.

## Docking Studies

The previously developed rTSPO model<sup>24</sup>, generated based on the published mouse solution structure of TSPO (PDB code 2MGY),<sup>39</sup> was used to dock compound **6** and **7-12**. These studies were performed employing the Glide tool implemented in Maestro 9.8.<sup>40</sup> The 3D structures of compound **6** and **7-12** were generated with the Maestro fragment Build tool and then geometrically optimized with Macromodel.<sup>40</sup> Herein we used the rTSPO structure obtained in our previous work<sup>21</sup> and prepared through the Protein Preparation Wizard of the Maestro 9.8<sup>40</sup> graphical user interface which assigns bond orders, adds hydrogen atoms, and generates appropriate protonation states.

The docking grid box was centered on the residues lining the binding pocket of **1**, with a grid box dimension equal to 24 Å × 24 Å × 24 Å. The residues considered to center the docking grid are A23, V26, L49, A50, I52, W107, V110, L114, A147, and L150 (which are conserved between the mTSPO and rTSPO, apart from A110V). Finally, docking runs were carried out using the standard precision (SP) method. Pictures were rendered employing the UCSF Chimera software.<sup>41</sup>

## Biological Evaluation.

**[<sup>3</sup>H]-1 Displacement and Competition Kinetic Association Assays.** Both the radioligand binding assays were performed on rat kidneys membranes prepared as previously described.<sup>42</sup> The resulting membrane pellets were frozen at -20 °C. All the experimental procedures were carried out following the guidelines of the European Community Council Directive 86-609 and have been approved by the Committee for animal experimentation of the University of Pisa. For both radioligand binding assays, an aliquot of membranes was thawed, suspended in Assay Buffer (AB, Tris-HCl 50 mM, pH 7.4), and homogenized using Ultraturrax. Protein content in cell homogenate was measured by the Bradford method.<sup>43</sup>

[<sup>3</sup>H]-1 displacement assay was performed as previously reported.<sup>32</sup> Briefly, membrane homogenates (20 µg of proteins) were incubated with increasing concentrations of each tested TSPO ligand and 1 nM [<sup>3</sup>H]-1 (85.7 µCi/nmol specific activity, Perkin-Elmer Life Sciences) in AB

(500  $\mu\text{L}$  final volume) for 90 min at 0  $^{\circ}\text{C}$ . Nonspecific [ $^3\text{H}$ ]-1 binding was determined in the presence of 1  $\mu\text{M}$  **1**; (Sigma-Aldrich). After the incubation time, samples were filtered with 3 mL of AB under vacuum through GF/C glass fiber filters. After being washed three times, radioactivity trapped on the filter was measured by liquid scintillation counter (TopCount; PerkinElmer Life and Analytical Sciences; 65% counting efficiency). For the active compounds, the ligand concentration that inhibited [ $^3\text{H}$ ]-1 binding to membranes by 50% ( $\text{IC}_{50}$  value) obtained from the inhibition curve was converted to  $K_i$  value using the method of Cheng and Prusoff.<sup>44</sup>

[ $^3\text{H}$ ]-1 competition kinetic association assay was performed as previously described.<sup>32</sup> Briefly, [ $^3\text{H}$ ]-1 was added simultaneously with the tested ligand to membrane homogenates (30  $\mu\text{g}$  of proteins) in a final volume of 500  $\mu\text{L}$  of AB. The [ $^3\text{H}$ ]-1 binding was assessed at multiple time points by filtration harvesting and liquid scintillation counting. The assay was performed using concentration of ligands corresponding to 3-fold their  $K_i$ .

**Fluorescent labeling of human glioblastoma cell line U343.** U343 human glioblastoma cells were plated on glass coverslip to a density of  $7 \times 10^4/500$   $\mu\text{L}$  well in 24-well plates. Cells were cultured in minimum essential medium Eagle with 2 mM L-glutamine and Earle's BSS adjusted to contain 1.5 g/L sodium bicarbonate and supplemented with 10% fetal bovine serum (FBS, Euroclone, Milan, Italy), 100 U/mL penicillin, 100 mg/mL streptomycin, 1% non-essential amino acids and 1.0 mM sodium pyruvate at 37  $^{\circ}\text{C}$  in 5%  $\text{CO}_2$ . Cells were grown to subconfluence and treated with different concentrations (3, 4, 5, 6 and 10  $\mu\text{M}$ ) of compound **15** or **16** for 30 min at 37  $^{\circ}\text{C}$ . Glioblastoma cells on coverslip were washed twice in PBS, fixed in paraformaldehyde (PFA) 4%. DAPI was used to counterstain nuclei. Slides were observed using a Zeiss LSM 710 Laser Scanning Microscope (Carl Zeiss MicroImaging GmbH). Samples were vertically scanned from the bottom of the coverslip with a 63 $\times$  (1.40 NA) Plan-Apochromat oil-immersion objective. Images were generated with Zeiss ZEN Confocal Software (Carl Zeiss MicroImaging GmbH).

**U343 staining with MitoTracker Red and compounds 15 and 16.** U343 subconfluent cells were treated with MitoTracker Red CMXRos (Invitrogen, Milano, Italy) at the final concentration of 200

1  
2  
3 nM for 1 h at 37 °C in 5% CO<sub>2</sub>, and subsequently with 5 μM of compound **15** or **16** for 30 min at 37  
4 °C in 5% CO<sub>2</sub>, while avoiding light bleaching. Coverslip slides have been processed as described  
5 above, and images were acquired using a 120× Plan-Apochromat oil-immersion objective.  
6  
7

8  
9 **Fluorescent labeling of human glioblastoma cell line U343 in the presence of 1.** U343  
10 subconfluent cells were preincubated with 10 μM or 50 μM of **1** for 30 min at 37 °C in 5% CO<sub>2</sub>,  
11 and then treated with different concentrations of compound **15** or **16** (0.1, 0.5, 1, 5 and 10 μM) for  
12 30 min at 37 °C. Coverslip slides have been processed as described above, and images were  
13 acquired using a 63× Plan-Apochromat oil-immersion objective.  
14  
15  
16  
17  
18  
19

20 **Cell Viability Assay.** Cell viability was determined using the 3-[4,5-dimethylthiazol-2,5-diphenyl-  
21 2*H*-tetrazolium bromide (MTT) colorimetric assay. Briefly, cells were seeded into 96-well plates to  
22 a density of 10<sup>4</sup>/100 μL/well. After 24 h of growth to allow attachment to the wells, compound **15**  
23 or **16** were added at various concentrations (from 0.1 to 10 μM). After 1, 2 and 4 h 10 μL MTT (5  
24 mg/mL) was added to each well, and cells were incubated in the dark for 2 h (37 °C, 5% CO<sub>2</sub>).  
25 When dark crystals appeared at the well bottom, the solution was then gently aspirated from each  
26 well, and the formazan crystals were dissolved with 100 μL of DMSO, yielding a purple solution.  
27 Optical densities were read at 550 nm using a Multiskan Spectrum Thermo Electron Corporation  
28 reader.  
29  
30  
31  
32  
33  
34  
35  
36  
37  
38  
39  
40  
41  
42

### 43 **Supporting Information.**

44  
45  
46 The Supporting Information is available free of charge on the ACS Publications website at  
47 <http://pubs.acs.org>.  
48  
49

50  
51 <sup>1</sup>H NMR and <sup>13</sup>C NMR of compounds **8-16**, effect of compounds **15** and **16** on cell viability (PDF).  
52  
53

54 SMILES molecular formula strings (CSV)  
55  
56  
57  
58  
59  
60

### Corresponding Author

\* To whom all correspondence should be addressed. S. Cosconati, Tel: 39 0823274789. Fax: 39 0823274585. E-mail: sandro.cosconati@unicampania.it; S. Castellano, Tel: 39 089969244. Fax: 39 089969602. E-mail: scastellano@unisa.it; S. Taliani, Tel: 39 0502219547. Fax: 39 0502219605; E-mail: sabrina.taliani@unipi.it.

### Author Contributions

The manuscript was written through contributions of all authors. All authors have given approval to the final version of the manuscript. ‡ These authors contributed equally.

### Acknowledgment

This study was financially supported by grants from Regione Campania (Italy, Grants 2007 and 2008 LR 5/02) and from the Universities of Pisa and Salerno (Italy).

### Abbreviations

NBD, 7-nitro-2,1,3-benzoxadiazol-4-yl; PBS, phosphate buffered saline; PET, positron emission tomography; RT, Residence Time; TFA, trifluoroacetic acid; TSPO, Translocator Protein.

### References

1. Heneka, M. T.; Rodriguez, J. J.; Verkhratsky, A. Neuroglia in neurodegeneration. *Brain Res. Rev.* **2010**, *63*, 189-211.
2. Papadopoulos, V.; Baraldi, M.; Guilarte, T. R.; Knudsen, T. B.; Lacapere, J. J.; Lindemann, P.; Norenberg, M. D.; Nutt, D.; Weizman, A.; Zhang, M. R.; Gavish, M. Translocator protein (18 kDa): new nomenclature for the peripheral-type benzodiazepine receptor based on its structure and molecular function. *Trends Pharmacol. Sci.* **2006**, *27*, 402-409.

- 1  
2  
3 3. Chen, M. K.; Guilarte, T. R. Translocator protein 18 kDa (TSPO): molecular sensor of brain  
4 injury and repair. *Pharmacol. Ther.* **2008**, *118*, 1-17.  
5  
6
- 7  
8 4. Liu, G. J.; Middleton, R. J.; Hatty, C. R.; Kam, W. W.; Chan, R.; Pham, T.; Harrison-Brown,  
9 M.; Dodson, E.; Veale, K.; Banati, R. B. The 18 kDa translocator protein, microglia and  
10 neuroinflammation. *Brain Pathol.* **2014**, *24*, 631-653.  
11  
12
- 13 5. Papadopoulos, V.; Aghazadeh, Y.; Fan, J.; Campioli, E.; Zirkin, B.; Midzak, A. Translocator  
14 protein-mediated pharmacology of cholesterol transport and steroidogenesis. *Mol. Cell.*  
15 *Endocrinol.* **2015**, *408*, 90-98.  
16  
17
- 18 6. Rupprecht, R.; Papadopoulos, V.; Rammes, G.; Baghai, T. C.; Fan, J.; Akula, N.; Groyer, G.;  
19 Adams, D.; Schumacher, M. Translocator protein (18 kDa) (TSPO) as a therapeutic target for  
20 neurological and psychiatric disorders. *Nat. Rev. Drug Discovery* **2010**, *9*, 971-988.  
21  
22
- 23 7. Li, F.; Liu, J.; Liu, N.; Kuhn, L. A.; Garavito, R. M.; Ferguson-Miller, S. Translocator protein  
24 18 kDa (TSPO): an old protein with new functions? *Biochemistry* **2016**, *55*, 2821-2831.  
25  
26
- 27 8. Guo, Y.; Kalathur, R. C.; Liu, Q.; Kloss, B.; Bruni, R.; Ginter, C.; Kloppmann, E.; Rost, B.;  
28 Hendrickson, W. A. Protein structure. Structure and activity of tryptophan-rich TSPO proteins.  
29 *Science* **2015**, *347*, 551-555.  
30  
31
- 32 9. Morohaku, K.; Pelton, S. H.; Daugherty, D. J.; Butler, W. R.; Deng, W.; Selvaraj, V.  
33 Translocator protein/peripheral benzodiazepine receptor is not required for steroid hormone  
34 biosynthesis. *Endocrinology* **2014**, *155*, 89-97.  
35  
36
- 37 10. Tu, L. N.; Morohaku, K.; Manna, P. R.; Pelton, S. H.; Butler, W. R.; Stocco, D. M.; Selvaraj,  
38 V. Peripheral benzodiazepine receptor/translocator protein global knock-out mice are viable  
39 with no effects on steroid hormone biosynthesis. *J. Biol. Chem.* **2014**, *289*, 27444-27454.  
40  
41  
42  
43  
44  
45  
46  
47  
48  
49  
50  
51  
52  
53  
54  
55  
56  
57  
58  
59  
60

- 1  
2  
3 11. Banati, R. B.; Middleton, R. J.; Chan, R.; Hatty, C. R.; Kam, W. W.; Quin, C.; Graeber, M. B.;  
4 Parmar, A.; Zahra, D.; Callaghan, P.; Fok, S.; Howell, N. R.; Gregoire, M.; Szabo, A.; Pham,  
5 T.; Davis, E.; Liu, G. J. Positron emission tomography and functional characterization of a  
6 complete PBR/TSPO knockout. *Nat. Commun.* **2014**, *5*, 5452.  
7  
8  
9  
10  
11  
12 12. Batarseh, A.; Papadopoulos, V. Regulation of translocator protein 18 kDa (TSPO) expression  
13 in health and disease states. *Mol. Cell. Endocrinol.* **2010**, *327*, 1-12.  
14  
15  
16  
17  
18 13. Braestrup, C.; Squires, R. F. Specific benzodiazepine receptors in rat brain characterized by  
19 high-affinity (<sup>3</sup>H)diazepam binding. *Proc. Natl. Acad. Sci. U. S. A.* **1977**, *74*, 3805-3809.  
20  
21  
22  
23 14. Le Fur, G.; Guilloux, F.; Rufat, P.; Benavides, J.; Uzan, A.; Renault, C.; Dubroeuq, M. C.;  
24 Gueremy, C. Peripheral benzodiazepine binding sites: effect of PK11195, 1-(2-chlorophenyl)-  
25 *N*-methyl-(1-methylpropyl)-3-isoquinolinecarboxamide. II. In vivo studies. *Life Sci.* **1983**, *32*,  
26 1849-1856.  
27  
28  
29  
30  
31  
32  
33 15. Okubo, T.; Yoshikawa, R.; Chaki, S.; Okuyama, S.; Nakazato, A. Design, synthesis, and  
34 structure-activity relationships of novel tetracyclic compounds as peripheral benzodiazepine  
35 receptor ligands. *Bioorg. Med. Chem.* **2004**, *12*, 3569-3580.  
36  
37  
38  
39  
40  
41 16. Imaizumi, M.; Briard, E.; Zoghbi, S. S.; Gourley, J. P.; Hong, J.; Fujimura, Y.; Pike, V. W.;  
42 Innis, R. B.; Fujita, M. Brain and whole-body imaging in nonhuman primates of [<sup>11</sup>C]PBR28, a  
43 promising PET radioligand for peripheral benzodiazepine receptors. *NeuroImage* **2008**, *39*,  
44 1289-1298.  
45  
46  
47  
48  
49  
50  
51 17. Denora, N.; Laquintana, V.; Pisu, M. G.; Dore, R.; Murru, L.; Latrofa, A.; Trapani, G.; Sanna,  
52 E. 2-Phenyl-imidazo[1,2-*a*]pyridine compounds containing hydrophilic groups as potent and  
53 selective ligands for peripheral benzodiazepine receptors: synthesis, binding affinity and  
54 electrophysiological studies. *J. Med. Chem.* **2008**, *51*, 6876-6888.  
55  
56  
57  
58  
59  
60

- 1  
2  
3 18. Vivash, L.; O'Brien, T. J. Imaging microglial activation with TSPO PET: lighting up  
4  
5 neurologic diseases? *J. Nucl. Med.* **2016**, *57*, 165-168.  
6  
7  
8  
9 19. Primofiore, G.; Da Settimo, F.; Taliani, S.; Simorini, F.; Patrizi, M. P.; Novellino, E.; Greco,  
10  
11 G.; Abignente, E.; Costa, B.; Chelli, B.; Martini, C. *N,N*-dialkyl-2-phenylindol-3-  
12  
13 ylglyoxylamides. a new class of potent and selective ligands at the peripheral benzodiazepine  
14  
15 receptor. *J. Med. Chem.* **2004**, *47*, 1852-1855.  
16  
17  
18 20. Da Settimo, F.; Simorini, F.; Taliani, S.; La Motta, C.; Marini, A. M.; Salerno, S.; Bellandi, M.;  
19  
20 Novellino, E.; Greco, G.; Cosimelli, B.; Da Pozzo, E.; Costa, B.; Simola, N.; Morelli, M.;  
21  
22 Martini, C. Anxiolytic-like effects of *N,N*-dialkyl-2-phenylindol-3-ylglyoxylamides by  
23  
24 modulation of translocator protein promoting neurosteroid biosynthesis. *J. Med. Chem.* **2008**,  
25  
26 *51*, 5798-5806.  
27  
28  
29  
30 21. Barresi, E.; Bruno, A.; Taliani, S.; Cosconati, S.; Da Pozzo, E.; Salerno, S.; Simorini, F.;  
31  
32 Daniele, S.; Giacomelli, C.; Marini, A. M.; La Motta, C.; Marinelli, L.; Cosimelli, B.;  
33  
34 Novellino, E.; Greco, G.; Da Settimo, F.; Martini, C. Deepening the topology of the  
35  
36 translocator protein binding site by novel *N,N*-dialkyl-2-arylindol-3-ylglyoxylamides. *J. Med.*  
37  
38 *Chem.* **2015**, *58*, 6081-6092.  
39  
40  
41  
42 22. Daniele, S.; La Pietra, V.; Barresi, E.; Di Maro, S.; Da Pozzo, E.; Robello, M.; La Motta, C.;  
43  
44 Cosconati, S.; Taliani, S.; Marinelli, L.; Novellino, E.; Martini, C.; Da Settimo, F. Lead  
45  
46 Optimization of 2-phenylindolylglyoxylyldipeptide murine double minute  
47  
48 (MDM)2/translocator protein (TSPO) dual inhibitors for the treatment of gliomas. *J. Med.*  
49  
50 *Chem.* **2016**, *59*, 4526-4538.  
51  
52  
53  
54 23. Castellano, S.; Taliani, S.; Milite, C.; Pugliesi, I.; Da Pozzo, E.; Rizzetto, E.; Bendinelli, S.;  
55  
56 Costa, B.; Cosconati, S.; Greco, G.; Novellino, E.; Sbardella, G.; Stefancich, G.; Martini, C.;  
57  
58 Da Settimo, F. Synthesis and biological evaluation of 4-phenylquinazoline-2-carboxamides  
59  
60

- 1  
2  
3 designed as a novel class of potent ligands of the translocator protein. *J. Med. Chem.* **2012**, *55*,  
4  
5 4506-4510.  
6  
7
- 8  
9 24. Castellano, S.; Taliani, S.; Viviano, M.; Milite, C.; Da Pozzo, E.; Costa, B.; Barresi, E.; Bruno,  
10  
11 A.; Cosconati, S.; Marinelli, L.; Greco, G.; Novellino, E.; Sbardella, G.; Da Settimo, F.;  
12  
13 Martini, C. Structure-activity relationship refinement and further assessment of 4-  
14  
15 phenylquinazoline-2-carboxamide translocator protein ligands as antiproliferative agents in  
16  
17 human glioblastoma tumors. *J. Med. Chem.* **2014**, *57*, 2413-2428.  
18  
19
- 20  
21 25. Taliani, S.; Simorini, F.; Sergianni, V.; La Motta, C.; Da Settimo, F.; Cosimelli, B.; Abignente,  
22  
23 E.; Greco, G.; Novellino, E.; Rossi, L.; Gremigni, V.; Spinetti, F.; Chelli, B.; Martini, C. New  
24  
25 fluorescent 2-phenylindolglyoxylamide derivatives as probes targeting the peripheral-type  
26  
27 benzodiazepine receptor: design, synthesis, and biological evaluation. *J. Med. Chem.* **2007**, *50*,  
28  
29 404-407.  
30  
31
- 32  
33 26. Taliani, S.; Da Pozzo, E.; Bellandi, M.; Bendinelli, S.; Pugliesi, I.; Simorini, F.; La Motta, C.;  
34  
35 Salerno, S.; Marini, A. M.; Da Settimo, F.; Cosimelli, B.; Greco, G.; Novellino, E.; Martini, C.  
36  
37 Novel irreversible fluorescent probes targeting the 18 kDa translocator protein: synthesis and  
38  
39 biological characterization. *J. Med. Chem.* **2010**, *53*, 4085-4093.  
40  
41
- 42  
43 27. Pike, V. W.; Taliani, S.; Lohith, T. G.; Owen, D. R.; Pugliesi, I.; Da Pozzo, E.; Hong, J.;  
44  
45 Zoghbi, S. S.; Gunn, R. N.; Parker, C. A.; Rabiner, E. A.; Fujita, M.; Innis, R. B.; Martini, C.;  
46  
47 Da Settimo, F. Evaluation of novel N<sup>1</sup>-methyl-2-phenylindol-3-ylglyoxylamides as a new  
48  
49 chemotype of 18 kDa translocator protein-selective ligand suitable for the development of  
50  
51 positron emission tomography radioligands. *J. Med. Chem.* **2011**, *54*, 366-373.  
52  
53
- 54  
55 28. Zanotti-Fregonara, P.; Zhang, Y.; Jenko, K. J.; Gladding, R. L.; Zoghbi, S. S.; Fujita, M.;  
56  
57 Sbardella, G.; Castellano, S.; Taliani, S.; Martini, C.; Innis, R. B.; Da Settimo, F.; Pike, V. W.  
58  
59 Synthesis and evaluation of translocator 18 kDa protein (TSPO) positron emission tomography  
60

- 1  
2  
3 (PET) radioligands with low binding sensitivity to human single nucleotide polymorphism  
4 rs6971. *ACS Chem. Neurosci.* **2014**, *5*, 963-971.  
5  
6  
7  
8  
9 29. Ikawa, M.; Lohith, T. G.; Shrestha, S.; Telu, S.; Zoghbi, S. S.; Castellano, S.; Taliani, S.; Da  
10 Settimo, F.; Fujita, M.; Pike, V. W.; Innis, R. B.  $^{11}\text{C}$ -ER176, a radioligand for 18-kDa  
11 translocator protein, has adequate sensitivity to robustly image all three affinity genotypes in  
12 human brain. *J. Nucl. Med.* **2017**, *58*, 320-325.  
13  
14  
15  
16  
17  
18 30. Leopoldo, M.; Lacivita, E.; Berardi, F.; Perrone, R. Developments in fluorescent probes for  
19 receptor research. *Drug Discovery Today* **2009**, *14*, 706-712.  
20  
21  
22  
23  
24 31. Copeland, R. A.; Pompliano, D. L.; Meek, T. D. Drug-target residence time and its implications  
25 for lead optimization. *Nat. Rev. Drug Discovery* **2006**, *5*, 730-739.  
26  
27  
28  
29 32. Costa, B.; Da Pozzo, E.; Giacomelli, C.; Barresi, E.; Taliani, S.; Da Settimo, F.; Martini, C.  
30 TSPO ligand residence time: a new parameter to predict compound neurosteroidogenic  
31 efficacy. *Sci. Rep.* **2016**, *6*, 18164.  
32  
33  
34  
35  
36  
37 33. Costa, B.; Da Pozzo, E.; Cavallini, C.; Taliani, S.; Da Settimo, F.; Martini, C. Long residence  
38 time at the neurosteroidogenic 18 kDa translocator protein characterizes the anxiolytic ligand  
39 XBD173. *ACS Chem. Neurosci.* **2016**, *7*, 1041-1046.  
40  
41  
42  
43  
44 34. Costa, B.; Cavallini, C.; Da Pozzo, E.; Taliani, S.; Da Settimo, F.; Martini, C. The anxiolytic  
45 etifoxine binds to TSPO Ro5-4864 binding site with long residence time showing a high  
46 neurosteroidogenic activity. *ACS Chem. Neurosci.* **2017**, *8*, 1448-1454.  
47  
48  
49  
50  
51  
52 35. Taliani, S.; Costa, B.; Da Pozzo, E.; Barresi, E.; Robello, M.; Cavallini, C.; Cosconati, S.; Da  
53 Settimo, F.; Novellino, E.; Martini, C. Residence time, a new parameter to predict  
54 neurosteroidogenic efficacy of translocator protein (TSPO) ligands: the case study of N,N-  
55 dialkyl-2-arylindol-3-ylglyoxylamides. *ChemMedChem* **2017**, doi: 10.1002/cmdc.201700220.  
56  
57  
58  
59  
60

1  
2  
3 Published online June 22, 2017.  
4  
5 <http://onlinelibrary.wiley.com/doi/10.1002/cmde.201700220/full> (accessed August 8, 2017).  
6  
7

- 8  
9 36. Uchiyama, S.; Santa, T.; Okiyama, N.; Fukushima, T.; Imai, K. Fluorogenic and fluorescent  
10 labeling reagents with a benzofurazan skeleton. *Biomed. Chromatogr.* **2001**, *15*, 295-318.  
11  
12  
13 37. Collado, D.; Perez-Inestrosa, E.; Suau, R.; Lopez Navarrete, J. T. Regioselective hydroxylation  
14 of phenols by simultaneous photochemical generation of phenol cation-radical and hydroxyl  
15 radical. *Tetrahedron* **2006**, *62*, 2927-2935.  
16  
17  
18  
19  
20  
21 38. Chalal, M.; Delmas, D.; Meunier, P.; Latruffe, N.; Vervandier-Fasseur, D. Inhibition of cancer  
22 derived cell lines proliferation by synthesized hydroxylated stilbenes and new ferrocenyl-  
23 stilbene analogs. Comparison with resveratrol. *Molecules* **2014**, *19*, 7850-7868.  
24  
25  
26  
27  
28  
29 39. Jaremko, L.; Jaremko, M.; Giller, K.; Becker, S.; Zweckstetter, M. Structure of the  
30 mitochondrial translocator protein in complex with a diagnostic ligand. *Science* **2014**, *343*,  
31 1363–1366.  
32  
33  
34  
35  
36  
37 40. *Maestro*, v. S. LLC: New York, <http://www.schrodinger.com/>, 2014.  
38  
39  
40 41. Pettersen, E. F.; Goddard, T. D.; Huang, C. C.; Couch, G. S.; Greenblatt, D. M.; Meng, E. C.;  
41 Ferrin, T. E. UCSF chimera--a visualization system for exploratory research and analysis. *J.*  
42 *Comput. Chem.* **2004**, *25*, 1605-1612.  
43  
44  
45  
46  
47 42. Chelli, B.; Salvetti, A.; Da Pozzo, E.; Rechichi, M.; Spinetti, F.; Rossi, L.; Costa, B.; Lena, A.;  
48 Rainaldi, G.; Scatena, F.; Vanacore, R.; Gremigni, V.; Martini, C. PK11195 differentially  
49 affects cell survival in human wild-type and 18 kDa translocator protein-silenced ADF  
50 astrocytoma cells. *J. Cell. Biochem.* **2008**, *105*, 712-723.  
51  
52  
53  
54  
55  
56  
57  
58  
59  
60

- 1  
2  
3 43. Bradford, M. M. A rapid and sensitive method for the quantitation of microgram quantities of  
4 protein utilizing the principle of protein-dye binding. *Anal. Biochem.* **1976**, 72, 248-254.  
5  
6  
7  
8 44. Cheng, Y.; Prusoff, W. H. Relationship between the inhibition constant ( $K_i$ ) and the  
9 concentration of inhibitor which causes 50 per cent inhibition ( $I_{50}$ ) of an enzymatic reaction.  
10  
11  
12 *Biochem. Pharmacol.* **1973**, 22, 3099-3108.  
13  
14  
15  
16  
17  
18

## Table of Contents Graphic

